EFFICIENT SOLUTIONS OF 2-D INCOMPRESSIBLE STEADY LAMINAR SEPARATED FLOWS

by

Joseph Hicks Morrison

Thesis submitted to the Faculty of the
Virginia Polytechnic Institute and State University
in partial fulfillment of the requirements for the degree of
MASTER OF SCIENCE
in
Aerospace Engineering

APPROVED:

Dr. B. Grossman, Chairman

Dr. J. A. Schetz

Dr. R. L. Simpson

February, 1986

Blacksburg, Virginia

EFFICIENT SOLUTION OF 2-D INCOMPRESSIBLE STEADY LAMINAR SEPARATED FLOWS

by

Joseph Hicks Morrison

Dr. B. Grossman, Chairman

Aerospace Engineering

Abstract

This thesis describes a simple efficient and robust numerical technique for solving two-dimensional incompressible laminar steady flows at moderate-to-high Reynolds numbers. The method uses an incremental multigrid method and an extrapolation procedure based on minimum residual concepts to accelerate the convergence rate of a robust block-line-Gauss-Seidel solver for the vorticity-stream function equations. Results are presented for the driven cavity flow problem using uniform and nonuniform grids and for the flow past a backward facing step in a channel.

ACKNOWLEDGEMENTS

The author has been supported under NASA training grant NGT 47-004-808. The author wishes to thank Dr. M. Napolitano of the Universite di Bari, Bari, Italy for his helpful discussions.

The author also wishes to thank Dr. B. Grossman for his assistance and patience during the time necessary to complete this work and Dr. D. L. Dwoyer and Pam Richardson of NASA Langley for their help.

The author also wishes to thank his wife, Kelly, for her patience and help.

TABLE OF CONTENTS

LIST OF FIGURES

LIST OF TABLES

NOMENCLATURE

ω	Vorticity
ψ	Stream Function
$\Delta( )$	Delta Formulation $\Delta( ) = ( )^{n+1} - ( )^{n}$
$\mathbf{f}$	Solution Vector $= (\omega, \psi)^{T}$
$\mathbf{R(f)}$	Residual Vector $= (R(\omega), R(\psi))^{T}$
C_h^H	Collection operator from h grid to H grid
I_H^h	Interpolation operator from H grid to h grid
$\kappa, \kappa_1, \kappa_2$	Parameters for extrapolation based on minimum residual
l, k	Parameters to control application of residual extrapolation
n	Unit normal vector
$\mathbf{q}$	Velocity vector
Re	Reynolds number
x, y	Cartesian coordinates
ξ, η	Generalized curvilinear coordinates
u	Velocity in x-direction
v	Velocity in y-direction
t	Time
$\alpha, \beta, \gamma, \sigma, \tau, J$	Scale factors of the transformation $(x, y) \rightarrow (\xi, \eta)$

SUPERSCRIPTS

n	Time level = n Δt
h	Finest grid level
H	Coarser grid level = 2h, 4h, 8h

I. INTRODUCTION

This thesis is concerned with the simulation of 2-D (two-dimensional) incompressible steady laminar separated flows at moderate-to-high Reynolds numbers (Re), using a simple efficient and robust numerical technique. Among the many numerical methods developed for the incompressible Navier-Stokes equations, those recently employed to solve computationally difficult problems, i.e., high Re steady separated flows, are very complex and sophisticated. For example: (i) Ghia et al. [1] use the already cumbersome coupled strongly-implicit procedure (SIP) inside the very involved full-approximation storage (FAS) multigrid algorithm of Brandt [2]; (ii) Schreiber and Keller [3] use a direct biharmonic solver embedded in a Newton iteration process. Furthermore, in both techniques the solution at a lower value of Re has to be effectively used to generate the solution at a higher value of Re. Therefore, it appears worthwhile to provide one more method which is very simple, but still as powerful and efficient as the best techniques available to date.

The vorticity-stream function formulation of the incompressible Navier-Stokes equations has been chosen as a test case for the proposed methodology as it provides a simpler formulation than either primitive variables or hybrid schemes. The vorticity-stream function formulation requires the solution of 2x2 block systems rather than the 4x4 block

system that primitive variables would require. A review of some of the important advances in incompressible laminar vorticity-stream function formulation Navier-Stokes solution procedures follows.

Rubin [4] gives an overview of different formulations of the incompressible Navier-Stokes equations and the reader is referred to his paper for a discussion of formulations other than vorticity-stream function such as primitive variables or hybrid schemes. He makes some observations of past experience with the vorticity-stream function and they are summarized here: (i) first-order upwinding converges rapidly to incorrect solutions due to numerical viscosity; (ii) coupling the vorticity and stream function equations provides faster convergence than any uncoupled method; (iii) combining a coupled algorithm with a multigrid scheme can significantly reduce computational time at the cost of increased storage. Various methods which have led to these observations are detailed below.

Rubin and Khosla [5] extended the strongly implicit procedure (SIP) of Stone [6] to solve a set of two coupled equations. They noted that the usual manner of solving the vorticity-stream function formulation of the Navier-Stokes equations, i.e. in an uncoupled manner by marching the vorticity transport equation in time and then solving the Poisson equation for the stream function (e.g. see Burrgraff [7] or Roache [8]), is very restrictive and time consuming as a nearly converged Poisson solution is required and a strict limit on time step exists even for

implicit time stepping. The SIP is a quasi-LU decomposition of the matrix formed from the spatial discretization and allows a complete coupling of the equations including boundary conditions. An important limitation of SIP is the large amount of storage required for the matrix inversion.

Rubin and Khosla used an upwind differencing scheme with correction for the advection term. The convective terms are split into an implicit upwind term and an explicit second-order correction term, which recovers a second order spatial accuracy at convergence to steady-state. This differencing is termed K-R differencing [9]. The boundary conditions are handled in an analogous manner. Second order accurate boundary conditions for the vorticity-stream function require the use of the boundary grid point and two grid points inside of the boundary. The SIP procedure only allows the implicit use of one grid point inside of the boundary and the boundary grid point, hence their method implements the boundary condition as a first order implicit scheme with a second-order explicit corrector to regain second-order accuracy in the converged steady-state solution. They applied this method to the driven cavity and to several other problems and achieved good results.

Ghia, Ghia and Shin [1] have extended the coupled strongly implicit procedure (CSIP) as described above with a multigrid method. The multigrid method that they implemented was the full approximation storage full multigrid (FAS-FMG) procedure of Brandt [2, 10] and Brandt

and Dinar [11]. The accomodative version of the FAS-FMG procedure was implemented such that a multigrid cycle is injected into the iterative solution (smoother in Brandt's terminology) whenever the convergence rate is not satisfactory. The concept behind a multigrid strategy is that any given mesh can only quickly annihilate those frequencies of errors which can be described on that grid. Thus, a fine mesh should only be used to annihalate small wavelength high frequency error components and that a coarser grid should be used to annihilate longer wavelength lower frequency errors. This is accomplished by caclulating a coarse grid correction to the fine grid results when the fine grid has annihalated the high frequency errors. This correction is interpolated back to the fine grid in such a manner as to minimize any high frequency errors that are introduced in the switching between grids. If the coarse grid does not converge satisfactorily, another multigrid cycle is injected switching to yet a coarser grid.

The collection (restriction) and interpolation (prolongation) operators used are the nine-point operators that will be used in this study and defined elsewhere in this paper. On the converged coarse grid, a cubic interpolation was used as suggested by Brandt [10] and Brandt and Dinar [11]. The FMG cycle begins by calculating a converged solution on the coarse grid and interpolating this to the next finer grid. This grid is then converged, injecting multigrid cycles where necessary, and then interpolated to the next finer grid until a converged solution is obtained on the desired finest grid. Ghia, Ghia

and Shin have reported that this process works well on the driven cavity problem as long as the coarse grid is not too coarse which may not not follow the physics and lead to an erroneous solution.

The use of the multigrid procedure further increases the memory requirements of the CSIP-MG method. The multigrid process leads to a much improved convergence rate especially as the grid is refined. The results were only for a driven cavity using a uniform mesh. Results were presented for grids as fine as 257 x 257 for Re up to 10,000 with a relatively small computation time.

Napolitano and Walters [12] have developed a line Gauss-Seidel (LGS) method for both the incompressible and compressible Navier-Stokes equations. The governing equations are discretized in time using a backward Euler time step and are linearized using the delta (Δ) formulation of [13]. The resulting set of equations can then use a different spatial discretization for the left hand side (LHS) implicit operator and the right hand side (RHS) residual. The LHS is discretized using first-order accurate upwind differencing for the first derivative terms and second-order accurate central differences elsewhere. This leads to a large sparse system which is solved approximatley at each time step by a line Gauss-Seidel sweep which requires only the solution of a block 2x2 tridiagonal system. The RHS is discretized using second order accurate central differences such that second-order spatial accuracy is recovered in the converged stead-state solution. The upwind

differences add an artificial viscosity term which vanishes in the steady-state and provides a diagonally dominant system to invert. This method requires minimal storage for the inversion routine.

For the driven cavity, Napolitano used alternating sweep directions of left-to-right followed by top-to-bottom for improved convergence. Napolitano [14] also applied this method to the cubic channel flow studied by several authors using Navier-Stokes and boundary layer equations [15 - 17] and achieved good accuracy and fair convergence, much better convergence than he reports for an alternating direction implicit (ADI) method [18].

Napolitano reports that the convergence of this method deteriorates as the mesh is refined. He developed an "incremental" multigrid scheme to address this issue [19]. He uses the LGS method as a smoother and a "cycling" multigrid strategy. Jameson [20] has shown the effectiveness of a cycling multigrid strategy as applied to the Euler equations. The strategy is to do a fixed number of iterations using the smoother on a grid and then to switch to the next coarser grid and repeat the process. Both the method of Jameson and Napolitano use one sweep of the smoother before switching to the next grid. Brandt [2] states that the advantage of the cycling versus accomodative procedure is in the saving of work in computing the switching criteria, replacing it instead with a fixed cycle. Napolitano has achieved encouraging results using this

incremental multigrid approach for the driven cavity problem. He presents results for the Re = 1000 case using a uniform grid.

Hafez and Cheng [21] have developed an extrapolation technique for iterative solvers based on the power method. The basic idea is to extrapolate two iterates of the solution to an improved guess of the solution. They applied this method to a line SOR scheme for transonic flow using transonic small disturbance theory. They achieved good results for this problem with the extrapolation technique.

More recently, Hafez et al. [22] have extended the extrapolation based on the power method to more parameters and introduced an extrapolation based on minimum residual techniques. These have been investigated on the multigrid Euler code of Jameson [20]. Both of these extrapolation techniques have been shown to improve convergence.

The work presented here is based on recent work by Napolitano [19], Napolitano and Walters [12] and Hafez et al. [22]. The vorticity-stream function formulation of the Navier-Stokes equations is chosen in two dimensions as a test for the proposed numerical method. While this may seem to be a very restrictive choice as the vorticity-stream function formulation does not easily extend to three dimensions, the basic solution method of the incremental multigrid scheme has been used by Napolitano for a model Laplace equation, vorticity-stream function

Navier-Stokes, and lambda formulation Euler equations. The line Gauss-Seidel solver has been applied to second-order upwinding for flux split compressible Euler and Navier-Stokes equations by several authors [23 - 25]. The extrapolation technique of Hafez has been applied to compressible Euler equations [22] and also to the transonic small disturbance equations [21]. Therefore, it is believed that the method applied here is easily and efficiently applied to other problems.

The basic method of Napolitano has been used only for uniform grids and will be extended here for nonuniform grids by implementing an appropriate weighting of the collection and interpolation functions based on the physical grid [26]. Improvements to convergence for the nonuniform grid similar to those achieved on the uniform grids will be shown. The method will be applied to higher Re driven cavity flows and to the backward facing step as calculated by Armaly et al. [27] and Kim and Moin [28]. All of these cases will be investigated using the residual extrapolation technique also and results will be presented showing from modest to sizeable increases in the convergence with the extrapolation.

Chapter II gives the governing equations for both uniform and nonuniform coordinates for the vorticity-stream function Navier-Stokes equations. Chapter III then details the numerical solution procedure with section 3.1 giving the discretization, section 3.2 the incremental multigrid scheme and section 3.3 the details of the one-parameter and

two-parameter residual extrapolation. Boundary conditions and their implementation are discussed in section 3.4. Chapter IV gives a discussion of results as applied to the driven cavity in uniform and nonuniform coordinates and to the backward facing step flow. Chapter V presents a summary of the method.

II. GOVERNING EQUATIONS

2.1 CARTESIAN COORDINATES

For a two-dimensional flow, the vorticity may be written in Cartesian coordinates as $\omega = \nabla \times q = \partial v/\partial x - \partial u/\partial y$ where q is the velocity vector and u and v are the x and y components of velocity respectively. The stream function in two-dimensional flow is defined as $u = \partial\psi/\partial y$ and $v = -\partial\psi/\partial x$, where the velocities have been nondimensionalized by a characteristic velocity, U_∞, and the lengths by a characteristic length, L. With these variables (ω, ψ), the Navier-Stokes equations in two dimensions may be written as:

$$\omega_t + \psi_y \omega_x - \psi_x \omega_y - (\omega_{xx} + \omega_{yy}) / Re = 0 \qquad (2.1)$$

$$\omega + \psi_{xx} + \psi_{yy} = 0 \qquad (2.2)$$

where the subscripts denote partial derivatives, t is time, x and y are the Cartesian coordinates and Re is the Reynolds number.

2.2 GENERALIZED CURVILINEAR COORDINATES

Transforming to a general curvilinear coordinate system

$$\xi = \xi(x,y)$$

$$\eta = \eta(x,y)$$

equations 2.1 and 2.2 may be written as:

$$(2.3) \quad \omega_t + (\psi_\eta \omega_\xi - \psi_\xi \omega_\eta) / J - (\alpha\omega_{\xi\xi} - 2\beta\omega_{\xi\eta} + \gamma\omega_{\eta\eta} + \sigma\omega_\eta + \tau\omega_\xi) / Re = 0$$

$$(2.4) \quad \omega + (\alpha\psi_{\xi\xi} - 2\beta\psi_{\xi\eta} + \gamma\psi_{\eta\eta} + \sigma\psi_\eta + \tau\psi_\xi) = 0$$

J, α, β, γ, σ, τ are the Jacobian and scale factors of the transformation. The scale factors are defined for a general stretching as:

$$\alpha = \left(\frac{1}{x_\xi} \right)^2 + \left(\frac{1}{y_\xi} \right)^2$$

$$\beta = - \left(\frac{1}{x_\xi x_\eta} + \frac{1}{y_\xi y_\eta} \right)$$

$$\gamma = \left(\frac{1}{x_\eta} \right)^2 + \left(\frac{1}{y_\eta} \right)^2$$

(2.5)

$$\sigma = - \frac{1}{x_\eta^2} \left(\frac{x_{\xi\eta}}{x_\xi} + \frac{x_{\eta\eta}}{x_\eta} \right) - \frac{1}{y_\eta^2} \left(\frac{y_{\xi\eta}}{y_\xi} + \frac{y_{\eta\eta}}{y_\eta} \right)$$

$$\tau = - \frac{1}{x_\xi^2} \left(\frac{x_{\xi\xi}}{x_\xi} + \frac{x_{\xi\eta}}{x_\eta} \right) - \frac{1}{y_\xi^2} \left(\frac{y_{\xi\xi}}{y_\xi} + \frac{y_{\xi\eta}}{y_\eta} \right)$$

$$\frac{1}{J} = \frac{1}{x_\xi \, y_\eta} - \frac{1}{x_\eta \, y_\xi}$$

III. NUMERICAL METHOD

3.1 DISCRETIZATION

Equations 2.1 and 2.2 are discretized in time using an implicit backwards Euler time stepping and are linearized using the delta approach neglecting terms of order Δ^2. The resulting equations may be written

$$
\begin{aligned}
(3.1)\quad & \Delta\omega/\Delta t + [\ \psi_y^n\, \Delta\omega_x + \omega_x^n\, \Delta\psi_y - \psi_x^n\, \Delta\omega_y - \omega_y^n\, \Delta\psi_x\ ] \\
& \quad - [\ \Delta\omega_{xx} + \Delta\omega_{yy}\ ] / Re \\
& = -[\ (\psi_y\, \omega)_x^n - (\psi_x\, \omega)_y^n\ ] + [\ \omega_{xx}^n + \omega_{yy}^n\ ] / Re \\
& = R(\omega^n)
\end{aligned}
$$

$$
\begin{aligned}
(3.2)\quad & \Delta\omega + [\ \Delta\psi_{xx} + \Delta\psi_{yy}] = -\omega^n - [\ \psi_{xx}^n + \psi_{yy}^n\ ] \\
& = R(\psi^n)
\end{aligned}
$$

Similarly, for a curvilinear coordinate system, the governing equations (Eqs. 2.3 and 2.4) are also discretized in time using a first-order accurate backwards Euler time stepping and are linearized using the delta approach neglecting terms of order Δ^2 resulting in

$$
\begin{aligned}
(3.3)\quad & \Delta\omega/\Delta t + [\ \psi^n_\eta\, \Delta\omega_\xi + \omega^n_\xi\, \Delta\psi_\eta - \psi^n_\xi\, \Delta\omega_\eta - \omega^n_\eta\, \Delta\psi_\xi\ ] / J - \\
& \qquad [\ \alpha\, \Delta\omega_{\xi\xi} + \gamma\, \Delta\omega_{\eta\eta} + \sigma\, \Delta\omega_\eta + \tau\, \Delta\omega_\xi\ ] / Re \\
& = -[\ (\psi_\eta\, \omega)^n_\xi - (\psi_\xi\, \omega)^n_\eta\ ] / J + \\
& \qquad [\ \alpha\, \omega^n_{\xi\xi} - 2\,\beta\, \omega^n_{\xi\eta} + \gamma\, \omega^n_{\eta\eta} + \sigma\, \omega^n_\eta + \tau\, \omega^n_\xi\ ] / Re \\
& = R(\omega^n)
\end{aligned}
$$

$$
\begin{aligned}
(3.4)\quad & \Delta\omega + [\ \alpha\, \Delta\psi_{\xi\xi} + \gamma\, \Delta\psi_{\eta\eta} + \sigma\, \Delta\psi_\eta + \tau\, \Delta\psi_\xi\ ] \\
& = -\omega^n - [\ \alpha\, \psi^n_{\xi\xi} - 2\,\beta\, \psi^n_{\xi\eta} + \gamma\, \psi^n_{\eta\eta} + \sigma\, \psi^n_\eta + \tau\, \psi^n_\xi\ ] \\
& = R(\psi^n).
\end{aligned}
$$

In equations 3.1 and 3.2 (3.3 and 3.4), (ω^n, ψ^n) are the known solutions at time (iteration) level t^n and $(\Delta\omega, \Delta\psi)$ are the unknowns to be computed. Notice that the conservation form of the advection terms has been used on the RHS residual equations [12]. The mixed derivative $(\ )_{\xi\eta}$ has been evaluated explicitly at the known time level and hence

does not appear in delta form. For an orthogonal grid as will be employed for the driven cavity, $\beta = 0$, so that the explicit evaluation of the mixed term does not enter.

Equations 3.1 and 3.2 (3.3 and 3.4) are discretized in space using a two-point first-order accurate upwind formula for the first derivatives of incremental variables in the vorticity equation ($\Delta\omega_\xi$, $\Delta\psi_\eta$, $\Delta\omega_\eta$, $\Delta\psi_\xi$) and second-order accurate central differences for all of the other spatial operators. The upwind terms provide a diagonally dominant system to be inverted and also generates an artificial viscosity term to stabilize the transient calculations. The artificial viscosity goes to zero as the steady state is reached.

3.2 INCREMENTAL MULTIGRID SCHEME

The upwinding provides a diagonally dominant, large 2x2 block-pentadiagonal system to be inverted at each iteration. This linear system is rewritten here in compact form as:

$$(3.5) \quad \mathbf{L}\,\Delta\mathbf{f} = \mathbf{R}(\mathbf{f})$$

where **L** is a large 2x2 block-pentadiagonal matrix, $\Delta\mathbf{f}$ is the sought solution vector

$$(3.6)\quad \Delta \mathbf{f} = [\, \Delta\omega_1, \Delta\psi_1, \cdots \Delta\omega_N, \Delta\psi_N \,]^T$$

and $\mathbf{R}(\mathbf{f})$ is the known residual vector, $(R(\omega^n), R(\psi^n))^T$, whose elements are the right hand sides of Eqs. (3.1 - 3.2) or Eqs. (3.3 - 3.4) evaluated at every grid point. In all of the methods provided in [12, 14, 18], L is replaced by either the product of two block-tridiagonal matrices [18] or by a matrix L_1 obtained from L by simply dropping its uppermost diagonal [14], which amounts to solving equation (3.5) approximately by a single block-LGS iteration. If an alternating direction LGS method is employed [12], at two successive time levels the ordering used to obtain L is changed so that L_1 neglects the contribution of the "east" and "south" grid points in the computational stencil, respectively. In all cases, after obtaining $\Delta\mathbf{f}$, the solution is updated as

$$(3.7)\quad \mathbf{f} \leftarrow \mathbf{f} + \Delta\mathbf{f}$$

L_1 and $\mathbf{R}(\mathbf{f})$ are recomputed using the updated $\mathbf{f}$ values and the process is repeated until convergence, i.e., when some norm of $\Delta\mathbf{f}$ or of $\mathbf{R}(\mathbf{f})$ is sufficiently small. The incremental multigrid method of [19] is described here for completeness and proceeds as follows:

$$(3.8)\quad L_1^h \, \Delta f^h = R(f)^h$$

$$(3.9)\quad f^h \leftarrow f^h + \Delta f^h$$

.
.
.

$$(3.10)\quad L_1^H \Delta f^H = R(f)^H = C_h^H R(f)^h$$

$$(3.11)\quad \Delta f^h = I_H^h \Delta f^H$$

$$(3.12)\quad f^h \leftarrow f^h + \Delta f^h$$

.
.
.

In Eqs. (3.8 - 3.12) the superscript h refers to the finest grid, whereas H refers to any of the coarser meshes and can thus be equal to 2h, 4h and 8h in the present study where at most four grid levels are used. Furthermore, L_1^H is the matrix obtained by simple injection from the matrix L_1^h, $R(f)^H$ is obtained from $R(f)^h$ by applying the standard 9-point collection operator (C_h^H) as many times as necessary to go from the finest mesh h to the current mesh H, and I_H^h is the standard bilinear

interpolation operator from the mesh H to the mesh h. Eqs. 3.10 - 3.12 are solved for each of the grid levels being used; 2h, 4h, 8h and 16h.

Notice that in the present multigrid method only the finest grid solution is computed and needs to be stored. Also, the incremental solution at any grid level, Δf^H is immediately used to obtain Δf^h (by standard bilinear interpolation) and to update the finest grid solution f^h, so that a single array is used for all of the Δf^H. Therefore, although this method increases the work of the collection and interpolation, it requires no additional storage for f or Δf than that required by the basic smoother.

In the present study, two modifications to the basic approach described above have been introduced in order to employ nonuniform grids: (i) the 9-point collection operator for the residual has been modified so as to use weighted areas in physical space; (ii) the bilinear interpolation operator has been modified so as to use distances among gridpoints in physical space, see e.g., [26].

The boundary conditions for the vorticity stream function formulation is in terms of a Neumann condition for ψ. This would require a complicated interpolation procedure if the true boundary conditions were implemented at every grid level. Since the multilevel scheme is written in terms of deltas of the variables, homogeneous boundary conditions are used at all coarse grid levels and the true

boundary conditions are included implicitly at only the finest grid. Any anticipated loss of convergence may be partially offset by including the true boundary conditions as an explicit postprocessor after each sweep on the coarse grid levels.

3.3 RESIDUAL EXTRAPOLATION

In order to further enhance the convergence rate of the method, the extrapolation technique based on minimum residual concepts proposed by Hafez et al. [22], can be used after every k iterations to obtain a new initial condition for the finest mesh solution. Such a technique is extremely simple to code, uses a negligible amount of CPU time and will be shown to provide a significant improvement in the efficiency of the calculations.

Following Hafez et al. [22], the extrapolation based on the minimum residual technique may be summarized below. Define an updated guess of the solution vector f^n as:

$$(3.13) \quad f^* = f^{n-1} + \kappa \left(f^n - f^{n-1} \right)$$

Calculate κ such that $R(f^*) \cdot R(f^*)$ is minimized. If a linear system is assumed, $R(f^*)$ may be written as:

$$(3.14) \quad R(f^*) = R^{n-1} + \kappa \left(R^n - R^{n-1} \right)$$

The inner product becomes

$$(3.15) \quad [R(f^*)]^2 = [R^{n-1} + \kappa \left(R^n - R^{n-1} \right)]^2$$

and

$$(3.16) \quad \kappa = \frac{R^{n-1} \cdot \left(R^n - R^{n-1} \right)}{\left(R^n - R^{n-1} \right) \cdot \left(R^n - R^{n-1} \right)}$$

An update to the solution vector is then made according to Eq. 3.13.

The two parameter residual extrapolation technique is an extension of this idea, where f^* may now be written as:

$$(3.17) \quad f^* = f^{n-1} + \kappa_1 \left(f^n - f^{n-1} \right) + \kappa_2 \left(f^{n-1} - f^{n-2} \right).$$

The residual equation now becomes

$$(3.18)\quad R(f^*) = R^{n-1} + \kappa_1 (R^n - R^{n-1}) + \kappa_2 (R^{n-1} - R^{n-2})$$

and, therefore

$$(3.19)\quad [R(f^*)]^2 = [R^{n-1} + \kappa_1 (R^n - R^{n-1}) + \kappa_2 (R^{n-1} - R^{n-2})]^2.$$

Minimizing Eq. 3.19 results in the following 2x2 matrix to solve for the extrapolation parameters κ_1 and κ_2:

$$(3.20)\quad \begin{bmatrix} a & b \\ b & c \end{bmatrix} \begin{bmatrix} \kappa_1 \\ \kappa_2 \end{bmatrix} = \begin{bmatrix} d \\ e \end{bmatrix}$$

where

$$a = (R^n - R^{n-1}) \cdot (R^n - R^{n-1})$$

$$b = (R^{n-1} - R^{n-2}) \cdot (R^n - R^{n-1})$$

$$c = (R^{n-1} - R^{n-2}) \cdot (R^{n-1} - R^{n-2})$$

$$d = R^{n-1} \cdot (R^n - R^{n-1})$$

$$e = R^{n-1} \cdot (R^{n-1} - R^{n-2})$$

The algorithm for implementing the residual extrapolation may be summarized as follows:

i) perform l iterations of the multigrid scheme

ii) calculate κ (or κ_1 and κ_2) from Eq. 3.16 (Eq. 3.20)

iii) evaluate f^* from Eq. 3.13 (Eq. 3.17)

iv) repeat steps i - iii with l replaced by k.

In this algorithm, l and k are two free parameters that may be chosen based on numerical experiment. It will be shown that the convergence of the solution is not overly sensitive to the choice of l or k.

3.4 BOUNDARY CONDITIONS

3.4.1 DRIVEN CAVITY

The driven cavity problem has been used by many authors as a test problem for evaluating numerical techniques and is used here as a first test of the current method on both a stretched and unstretched grid. Figure 1 shows the driven cavity and the appropriate boundary conditions. The top wall of the cavity moves at uniform velocity along

its own axis and all other walls are at rest. The boundary conditions are no flow through the walls and zero tangential velocity relative to the wall.

The no-slip boundary condition provides that ψ and ψ_n (where ψ_n is the normal derivative of ψ at the wall) vanish at all non-porous walls. These boundary conditions provide no direct boundary condition for the vorticity. A boundary condition for ω is derived from the physical boundary conditions from the definition of ω as $\omega = - \nabla^2\psi$ following Ghia et al. [1].

3.4.1.1 CARTESIAN COORDINATES

At the top, moving wall, of the driven cavity, $y = 1$ and $j = N$, the boundary condition may be written as:

$$\psi_N = 0 \tag{3.21}$$

$$\omega_N = - (\psi_{xx} + \psi_{yy}) = - \psi_{yy} \tag{3.22}$$

as $\psi_{xx} = 0$ along the top.

Using a central difference approximation for ψ_{yy} and introducing an image point one grid point outside of the computational domain, the vorticity on the top may be written as:

$$(3.23) \quad \omega_N = - (\psi_{N+1} - 2 \psi_N + \psi_{N-1}) / \Delta y^2$$

ψ_{N+1} is evaluated using a third-order accurate finite difference form of the normal derivative of ψ which is known at all boundaries from the no-slip condition

$$(3.24) \quad \psi_{y_N} = (2 \psi_{N+1} + 3 \psi_N - 6 \psi_{N-1} + \psi_{N-2}) / 6\Delta y$$

but $\psi_y = u = U_\infty$ along the top. Therefore, the two boundary conditions to be implemented are:

$$(3.25) \quad \omega_N = - (3 U_\infty \Delta y - \frac{1}{2} \psi_N + 4 \psi_{N-1} - \frac{1}{2} \psi_{N-2}) / \Delta y^2$$

$$(3.26) \quad \psi_N = 0$$

These must be written in delta form to be implemented in the numerical procedure. This may be done by writing each equation at time n and time n+1 and subtracting to give:

$$(3.27) \quad \Delta\omega_N = - (4 \Delta\psi_{N-1} - \frac{1}{2} \Delta\psi_{N-2}) / \Delta y^2$$

and

$$(3.28)\quad \Delta\psi_N = 0$$

Care must be exercised when implementing boundary conditions in delta form such that ω_N and ψ_N at the first step is correct, i.e. set $\omega_N^{initial} = -3\,U_\infty \Delta y$ and $\psi_N^{initial} = 0$. The same procedure is followed for the boundary conditions on the other walls.

3.4.1.2 GENERALIZED CURVILINEAR COORDINATES

A similar procedure is followed for the case of nonuniform grids with only minor changes due to the stretching. The vorticity on the top, ω_N, is now written as:

$$(3.29)\quad \omega_N = -\left(\alpha\,\psi_{\xi\xi} - 2\,\beta\,\psi_{\xi\eta} + \gamma\,\psi_{\eta\eta} + \sigma\,\psi_\eta + \tau\,\psi_\xi \right)$$

The stretching to be used is orthogonal such that β is identically zero. On the top, $v = 0 = -\psi_x = -\psi_\xi\,\xi_x$. Therefore $\psi_\xi = 0 =$ constant and $\psi_{\xi\xi} = 0$. Eq. 3.29 becomes

$$(3.30)\quad \omega_N = -\left(\gamma\,\psi_{\eta\eta} + \sigma\,\psi_\eta \right)$$

A second-order accurate central difference is used for $\psi_{\eta\eta}$ and a third-order accurate finite-difference representation is used for ψ_η to solve

for the image point. At the top, $u = \psi_y = \psi_\eta \eta_y = U_\infty$. Therefore, $\psi_\eta = y_\eta U_\infty$. Eq. 3.30 may finally be written as:

$$(3.31)\quad \omega_N = -\left(-\frac{7}{2}\gamma \psi_N + 4\gamma \psi_{N-1} - \frac{1}{2}\gamma \psi_{N-2} \right) / \Delta\eta^2 - \left(3\frac{\gamma}{\Delta\eta} + \sigma \right) y_\eta U_\infty$$

in delta form

$$(3.32)\quad \Delta\omega_N = -\left(4\gamma \Delta\psi_{N-1} - \frac{1}{2}\gamma \Delta\psi_{N-2} \right) / \Delta\eta^2$$

$$(3.33)\quad \Delta\psi_N = 0$$

where the initial conditions are

$$(3.34)\quad \omega_N = -\left(3\frac{\gamma}{\Delta\eta} + \sigma \right) y_\eta U_\infty$$

and

$$(3.35)\quad \psi_N = 0.$$

The boundary conditions for the other walls may be derived similarly.

This formulation has been shown to be second-order accurate (see Ghia et al. [1]). The boundary conditions add an extra term to the tridiagonal system to be inverted at the top and bottom of the matrix. This is simple to include in the tridiagonal solver and adds no more complexity to the inversion routine.

The stretching used for this case transforms a nonuniform grid in physical space to a uniform grid in computational space. It is the same stretching as used in [12].

$$(3.36)\quad \begin{pmatrix} x \\ y \end{pmatrix} = 0.5 + 0.5 \tanh \left[A_0 \begin{pmatrix} 2\xi-1 \\ 2\eta-1 \end{pmatrix} \right] / \tanh A_0 .$$

As the parameter A_0 is increased, more grid points are clustered near the walls and, as $A_0 \to 0$, a uniform grid is reclaimed.

Since the stretching is of the form

$$(3.37)\quad \begin{aligned} \xi &= \xi(x) \\ \eta &= \eta(y), \end{aligned}$$

a great simplification in the scale factors is realized. All scale factors are calculated analytically as:

$$\alpha = \frac{1}{x_\xi^2}$$

$$\beta = 0$$

$$\gamma = \frac{1}{y_\eta^2}$$

(3.38)

$$\sigma = - \frac{y_{\eta\eta}}{y_\eta} \gamma$$

$$\tau = - \frac{x_{\xi\xi}}{x_\xi} \alpha$$

$$J = x_\xi \, y_\eta$$

where

$$x_\xi = A_o \, \mathrm{sech}^2 [A_o (2\xi - 1)] / \tanh A_o$$

$$x_{\xi\xi} = - 4 A_o \tanh [A_o (2\xi - 1)] \, x_\xi$$

(3.39)

$$y_\eta = A_o \, \mathrm{sech}^2 [A_o (2\eta - 1)] / \tanh A_o$$

$$y_{\eta\eta} = - 4 A_o \tanh [A_o (2\eta - 1)] \, y_\eta .$$

3.4.2 BACKWARD FACING STEP

The backward facing step flow, studied experimentally and numerically by Armaly *et al.* [27] and numerically by Kim and Moin [28]

has also been studied as a test problem for the present methodology. Figure 2 shows a schematic of the flow field. The Reynolds number for this flow is defined in [27] as:

$$(3.40) \quad Re = \frac{V\ D}{\nu}$$

where V is two-thirds of the maximum inlet velocity and D is the hydraulic diameter of the inlet (small) channel and is equal to twice its height, D = 2h.

The boundary conditions for the top and the bottom walls are no-slip conditions and are of the same form as for the uniform driven cavity, as no stretching is used for this case, where ψ_N is constant but non-zero. The bottom half of the left boundary is also a no-slip wall.

The top half of the left boundary is specified as a parabolic inflow velocity profile given as:

$$(3.41) \quad \begin{aligned} u &= -24\ y_1^2 + 12\ y_1 \\ v &= 0 \end{aligned}$$

where y_1 is a new variable defined for convenience with its origin at centerline of the channel. Integrating the velocity distribution with respect to y_1, ψ may be written for the inflow plane as:

$$(3.42) \quad \psi = -8\, y_1^3 + 6\, y_1^2 + C$$

To evaluate the constant of integration, the stream function is matched at $y_1 = 0$ with the value of the stream function on the bottom half of the wall, i.e., $\psi = 0$. The constant of integration becomes zero and the stream function on the top of the computational space ($y_1 = 0.5$) is seen to be $\psi = 0.5$. The vorticity is evaluated at the inflow as:

$$(3.43) \quad \omega = -\frac{1}{\Delta y^2}\psi_{yy} - \frac{1}{\Delta x^2}\psi_{xx}$$

where ψ_{yy} is evaluated analytically from Eq. 3.42 and ψ_{xx} is evaluated with a second-order accurate one-sided finite difference to yield:

$$(3.44) \quad \omega = -\frac{1}{\Delta y^2}(12 - 48\, y_1) - \frac{1}{\Delta y^2}\left(\frac{7}{2}\psi_{1,j} + 4\,\psi_{2,j} - \frac{1}{2}\psi_{3,j}\right).$$

The outflow boundary condition is a fully developed flow and may be written as a Neumann condition in primitive variables as:

$$(3.45) \quad \begin{aligned} \partial u/\partial x &= 0 \\ \partial v/\partial x &= 0. \end{aligned}$$

The corresponding boundary conditions for the vorticity-stream function formulation are:

$$\partial\omega/\partial x = 0$$

(3.46)

$$\partial\psi/\partial x = 0.$$

These derivatives are evaluated using second-order accurate one-sided finite-difference formulas to give the boundary condition as:

$$\omega_{M,j} = \frac{4}{3}\omega_{M-1,j} - \frac{1}{3}\omega_{M-2.j} \quad (3.47)$$

$$\psi_{M,j} = \frac{4}{3}\psi_{M-1,j} - \frac{1}{3}\psi_{M-2.j} \quad (3.48)$$

and in delta form these may be written as:

$$\Delta\omega_{M,j} = \frac{4}{3}\Delta\omega_{M-1,j} - \frac{1}{3}\Delta\omega_{M-2.j} \quad (3.49)$$

$$\Delta\psi_{M,j} = \frac{4}{3}\Delta\psi_{M-1,j} - \frac{1}{3}\Delta\psi_{M-2.j}. \quad (3.50)$$

IV. RESULTS/DISCUSSION

4.1 Driven Cavity - Uniform Grid

The classical driven cavity flow at Re = 1000 was considered at first, using a 97 x 97 uniform grid, in order to assess the influence of the extrapolation technique based on minimum residual concepts of [22] on the basic multigrid method of [19]. Convergence histories are provided in figures 3, 4 and 5 using up to four grid levels. The (L_1 norm of the) vorticity residual is plotted versus the work units, one work unit being the CPU time required to complete a global iteration on the finest grid. Figure 3 refers to the basic scheme of [19] whereas figures 4 and 5 refer to the same scheme supplemented by one-parameter and two-parameter extrapolation performed every ten iterations. It clearly appears that the basic multigrid method provides a significant efficiency gain over the basic smoother (as already seen in [19]) and the extrapolation technique of [22] is very beneficial especially when using three and four grid levels. In order to study the influence of the interval of application of the extrapolation, k, calculations were also performed using four grid levels and the two-parameter extrapolation every 5, 15 and 20 iterations. The results, summarized in Table 1 as the work units necessary for the vorticity residual to reach

10^{-12}, show that the convergence rate is rather insensitive to the value of k.

4.2 Driven Cavity - Nonuniform Grid

The same problem has been also used to assess the performance of the present improved method for the case of a nonuniform grid. The value $A_0 = 1.4$ is employed for the stretching given in Eq. 3.36, which provides a considerable stretching near the walls, as seen in figure 6, where the 65 x 65 mesh in physical space is depicted.

A time step of 0.2 was used for this case as the multigrid method did not converge when using the unitary value used for all other calculations. The present results are given in figures 7 and 8 where the vorticity residual is plotted versus the work units for the case of the improved method without or with the two-parameter extrapolation, respectively.

The results are somewhat surprising insofar as the solution using three grid levels is less efficient than that using two grid levels. However, a significant improvement is obtained when using four grid levels. Also, the efficiency of the calculations is overall markedly lower than when using a uniform grid (see figures 3 and 5). This is

obviously due to the use of a smaller value of the time step. These results are rather unsatisfactory, insofar as it may appear that the method is not very suitable to handle nonuniform grids. Therefore, the more difficult Re = 3200 problem has also been considered in order to verify the robustness of the present method. The results obtained without and with the two-parameter extrapolation are given in figures 9 and 10 respectively. It appears that the convergence rate is much slower than for the easier Re = 1000 flow case and that the improvements achieved using the extrapolation technique are much less significant. However, it must be pointed out that a similar reduction in efficiency is obtained also for the case of the uniform 97 x 97 grid (the results of which are omitted for brevity). Furthermore, the modified multigrid approach is seen to be extremely effective insofar as a satisfactory convergence level (residual = 10^{-3}) is obtained in less than 800 work units when using four grid levels, while more than 3000 work units are needed by the single grid method.

As far as the accuracy of the present calculations is concerned, the maximum values of the stream function (ψ_M) and the vorticity at the center of the moving plate (ω_C) are given in Table 2, where they are compared with the very accurate results of Ghia et al. [1]. The agreement is excellent and shows that for both the Re = 1000 and the Re = 3200 flow-cases the present 65 x 65 nonuniform-grid solutions are more accurate than those obtained using a 97 x 97 uniform mesh. Finally, it has to be pointed out that the present approach appears to become less

competitive as Re increases, insofar as the four-grids, Re = 3200 flow case with acceleration require about ten CPU hours on a Perkin-Elmer 3230, using double-precision arithmetic, to drive the residual to 10^{-12}. However, one has to consider that all calculations have been started from rest and no parameter has ever been optimized. Furthermore, a single precision calculation which only drives the residual to 10^{-3}, for engineering accuracy, would require about 100 CPU minutes of the aforementioned minicomputer, an effort which is of the same order as that required by the much more sophisticated methods of [1] and [2].

4.3 Flow Past a Backward Facing Step

The flow past a backward facing step in a channel has been chosen by the organizers of a GAMM workshop as the test case for comparing a great number of codes for solving the incompressible Navier-Stokes equations. From the book which provides all the results presented at the workshop [29], it clearly appears that for Re = 500 or higher, most methods face convergence difficulties and/or need some kind of upwinding to handle the flow regions where convection dominates diffusion. Physically, as clearly shown by the very careful experiments of Armaly et al. [27], the structure of the flow becomes more and more complicated as Re increases: the flow, which always separates over the step, reattaches downstream at a distance which increases with Re, and, for

sufficiently high values of Re, a secondary separation region develops on the wall opposite to the step. For this problem, the basic methodology of [19] has been employed using uniform meshes of 49 x 49, 65 x 49, 81 x 49, and 97 x 49 gridpoints for the cases Re = 200, 400, 600 and 800 respectively, the downstream boundary condition being set at a distance from the step equal to 7.5, 10, 12.5 and 15 (the height of the channel is equal to 1 and that of the step is equal to 0.5).

In all cases, the solution was started from rest and convergence was obtained without any difficulty using again $\Delta t = 1$ and any number of grid levels up to and including four. Calculations were also performed using the one- and two-parameter residual extrapolation of [22] every 10 iterations. The convergence histories corresponding to the Re = 200 flow-case are shown in figures 11, 12 and 13. It clearly appears that the multigrid method of [19] works very nicely also for this problem and that the extrapolation technique provides dramatic improvements in the efficiency of the calculations, especially when using few grid levels. This result is not surprising insofar as the convergence history of the basic method is always very smooth (see figure 11), so that extrapolation can indeed provide a good estimate for the sought solution.

Similar results were obtained for Re = 400, 600 and 800. For the last most difficult case, convergence to 10^{-12} required 1400 work units

using four grid levels and the extrapolation, corresponding to a CPU time of 280 minutes on the Perkin-Elmer 3230.

A grid refinement study was done, doubling the number of grid points in both the x and y directions to evaluate the grid employed. Figures 14 and 15 show the lower and upper walls vorticity distributions obtained using 97 x 97, 131 x 97, 161 x 97 and 193 x 97 gridpoints for the Re = 200, 400, 600 and 800 flow-cases respectively. On the same figures, the results obtained using the coarser grids are also given as symbols. It appears that for the Re = 200 and 400 flow-cases grid convergence has been achieved, whereas for Re = 600 and Re = 800 further mesh refinement is probably warranted. Table 3 gives the locations of the reattachment point for the primary separation bubble (X1R) and of the separation and reattachment of the secondary separation bubble (X2S, X2R) for both grids.

The reattachment length of the main separation bubble (X1R - calculated on the fine grid) is plotted versus Re in figure 16. The present computations are compared to the experimental and computational results of Armaly et al. [27] and to the numerical results of Kim and Moin [28]. The numerical results of [27] were obtained using a first-order upwind-difference scheme. The experimental data suffer from three-dimensional effects at Re > 600 as reported in [27]. The present results show good agreement to the calculations of [28] which were obtained using a second-order-accurate fractional step method on the

primitive variables and good agreement with experimental results where three-dimensionality was not present.

It needs to be remarked that for all values of Re the far downstream values of the vorticity on the lower and upper walls should be 3 and -3 respectively. From the results of figures 14 and 15, one may thus believe that the outflow boundary conditions have not been imposed far enough downstream, especially for the higher values of Re. Therefore, the coarser grid computations were repeated for the cases Re = 200 and Re = 800, moving the outflow boundary condition location to x = 15 and x = 25 respectively and obviously increasing the number of longitudinal gridpoints to maintain the same value of Δx. The results for the vorticity on the lower and upper walls are given in figures 17 and 18 for Re = 200 with the outflow condition at x = 7.5 and x = 15 and for Re = 800 with the outflow condition at x = 15 and x = 25. The vorticity is always seen to tend to its asymptotic value correctly and the results obtained using different locations for the outflow boundary conditions are in agreement.

V. CONCLUSIONS

A simple efficient and robust method has been developed for solving 2-D incompressible steady laminar separated flows. A block-LGS iteration procedure is used as smoother within a very simple, though effective, incremental multigrid algorithm, supplemented by an extrapolation procedure based on minimum residual concepts. The basic multigrid technique has been extended through the use of interpolations and collections based on physical grid areas to treat nonuniform meshes. The extrapolation based on minimum residual concepts has been shown to give an increase in efficiency over the basic solver at a cost of additional storage. The one-parameter extrapolation has shown to give good results requiring less storage than the two-parameter extrapolation. Further gains in efficiency have been shown by using the two-parameter extrapolation.

The resulting technique has been tested versus the classical driven cavity flow at Re = 1000 and Re = 3200 and the flow past a backward facing step in a channel for Re = 200, 400, 600 and 800. The basic methods involved in the solution procedure have been applied to other problems such that it is believed that the method of solution would be applicable to many other problems of interest.

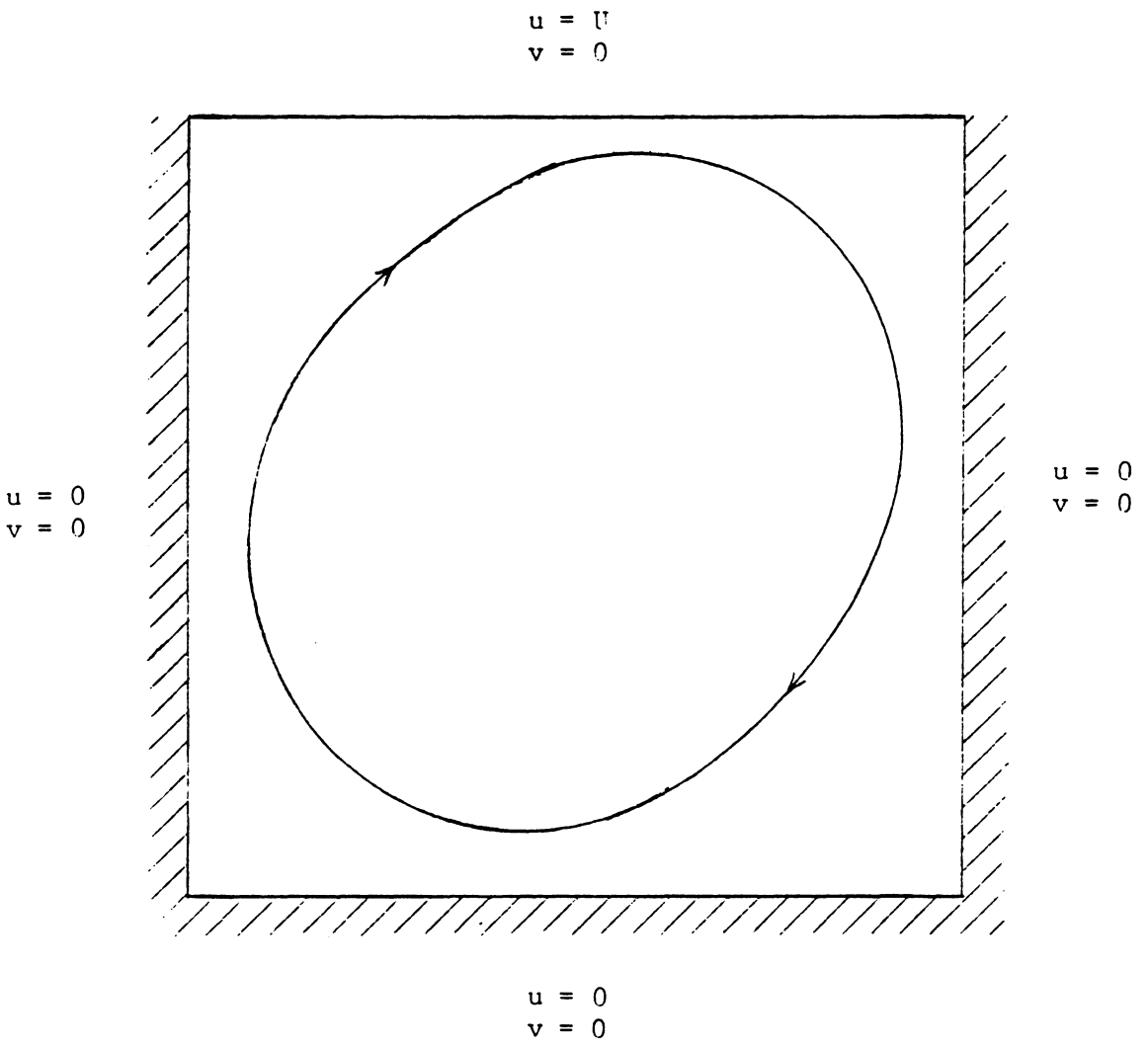

Fig. 1. Flow in a driven cavity

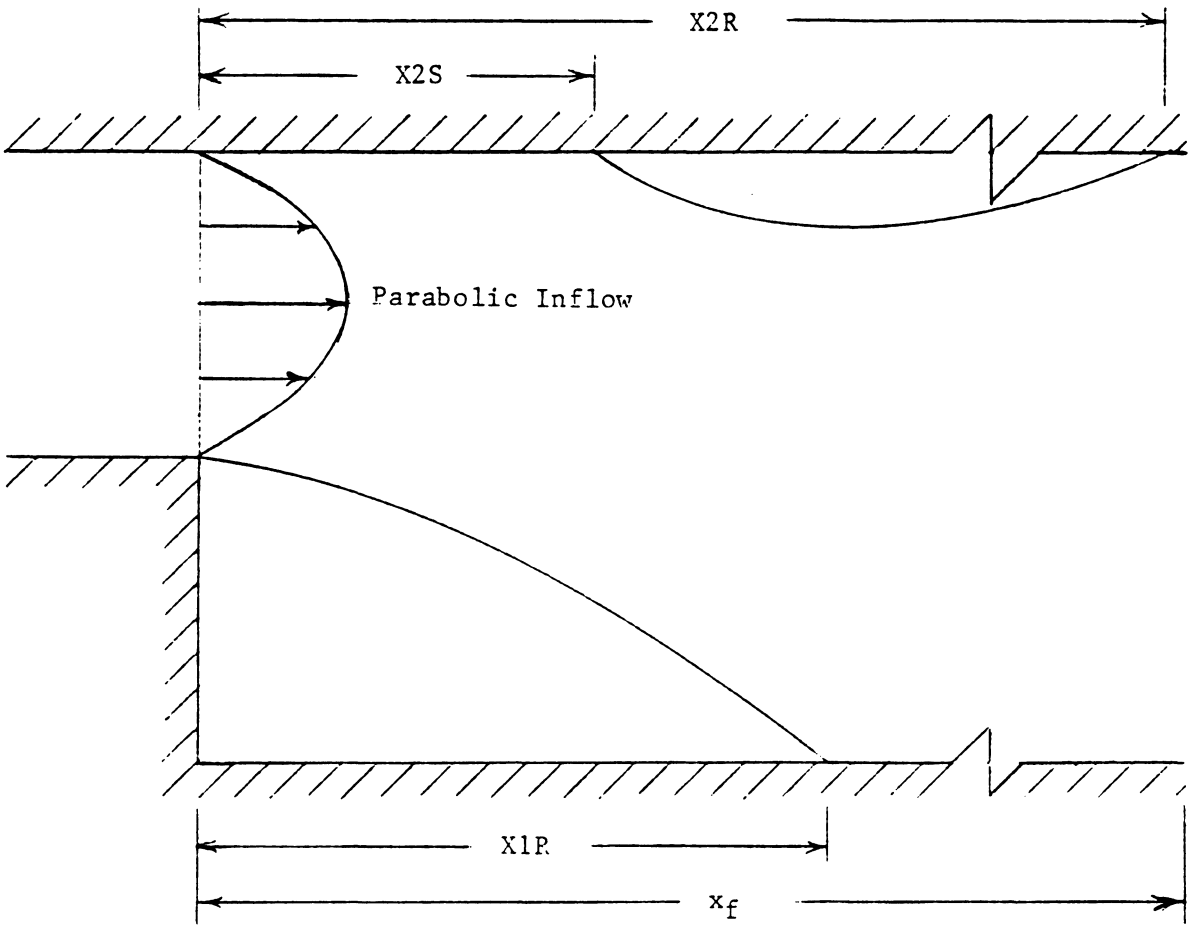

Fig. 2. Flow over a backward facing step
(1:2 expansion ratio)

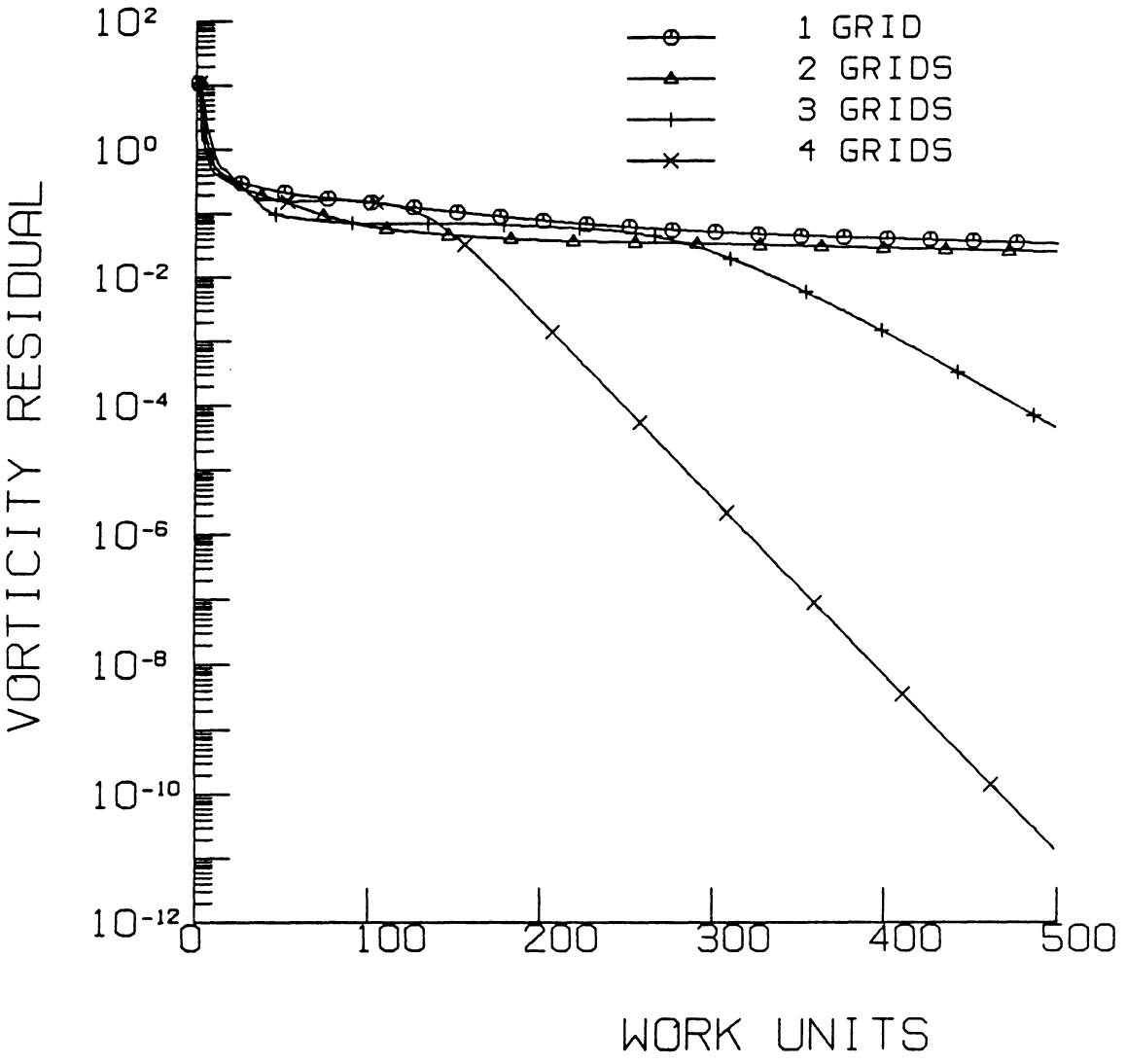

Fig. 3. Convergence history for driven cavity at Re = 1000, uniform 97 x 97 grid

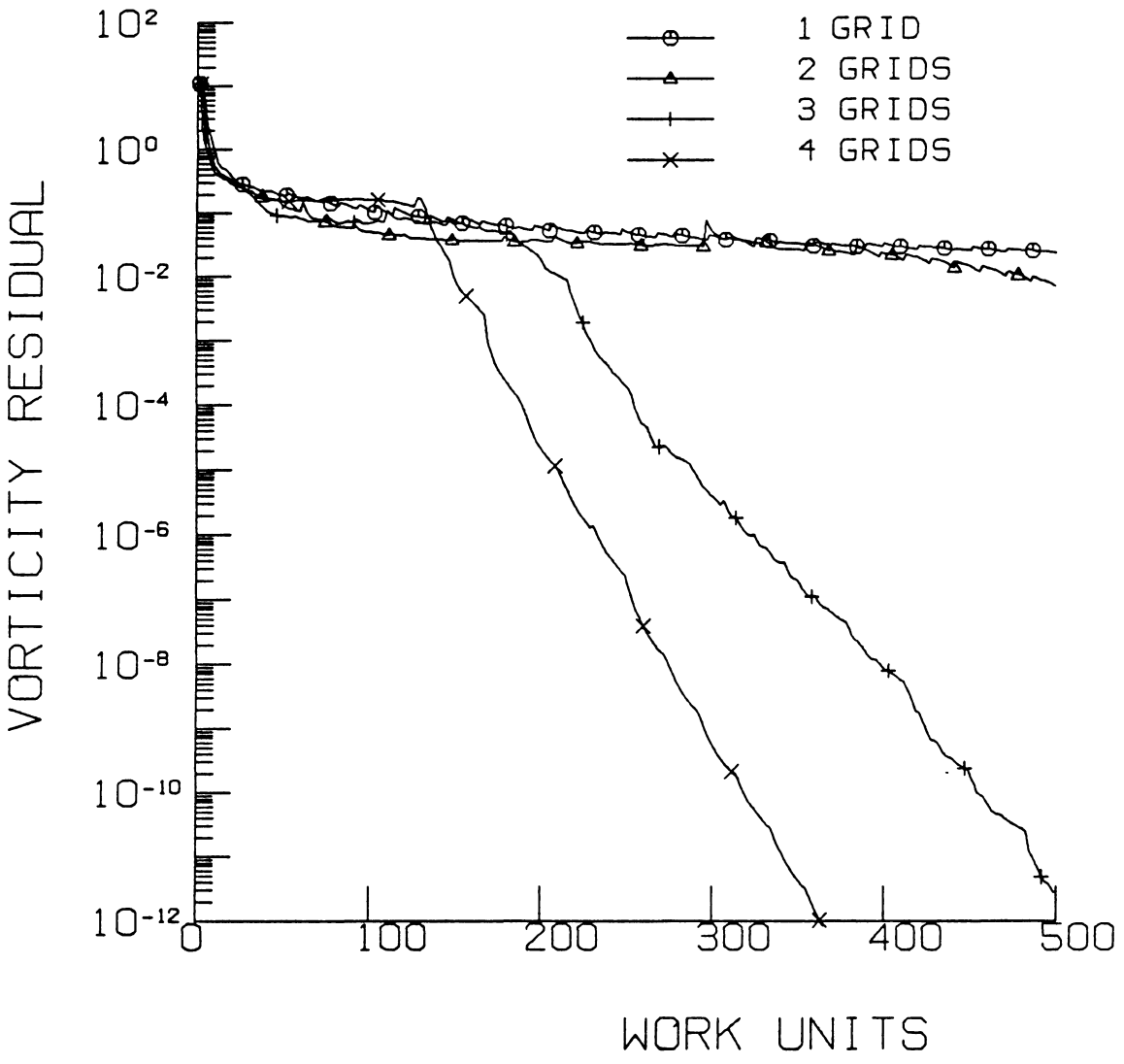

Fig. 4. Convergence history with one-parameter extrapolation for driven cavity at Re = 1000, uniform 97 x 97 grid

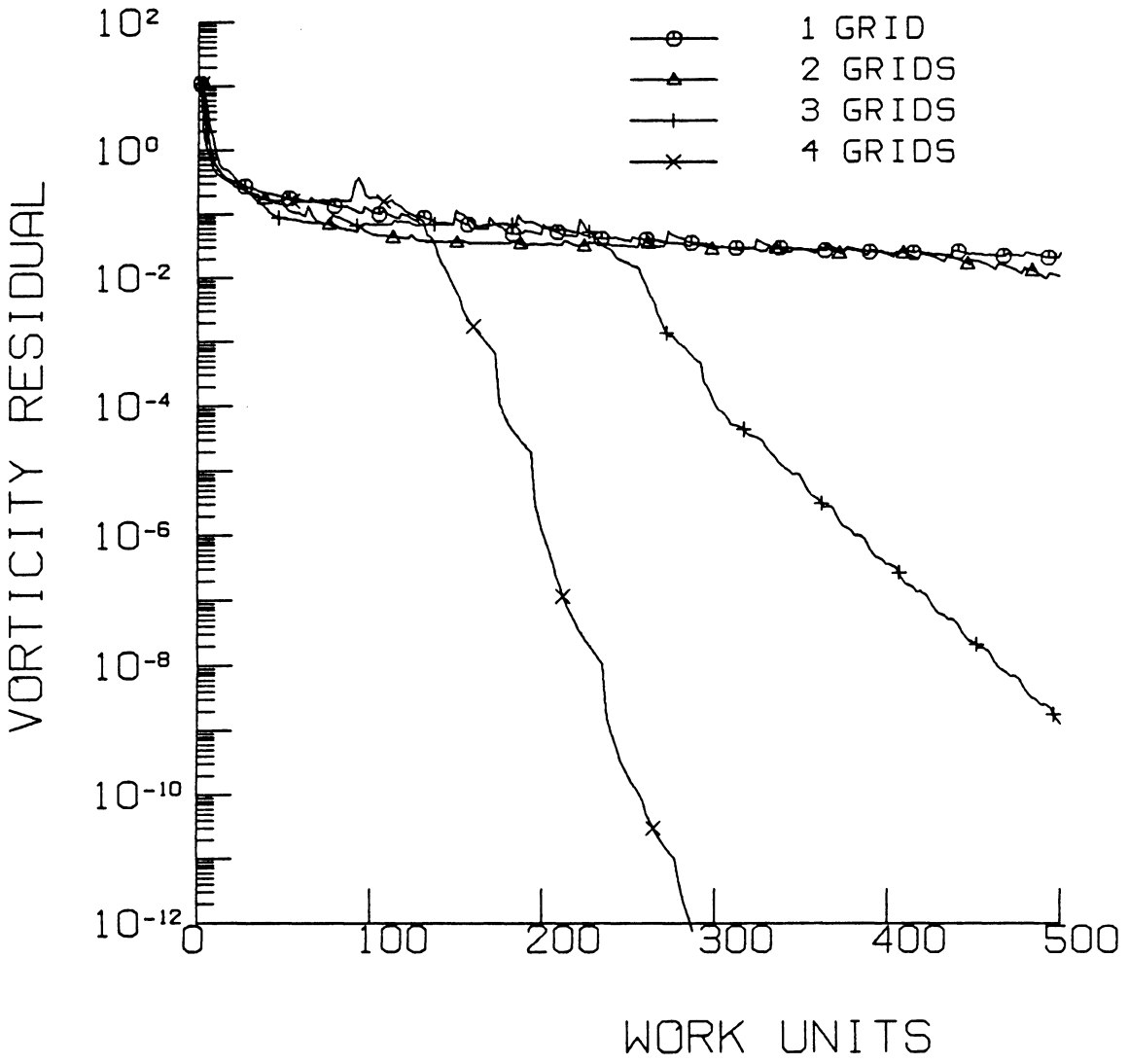

Fig. 5. Convergence history with two-parameter extrapolation for driven cavity at Re = 1000, uniform 97 x 97 grid

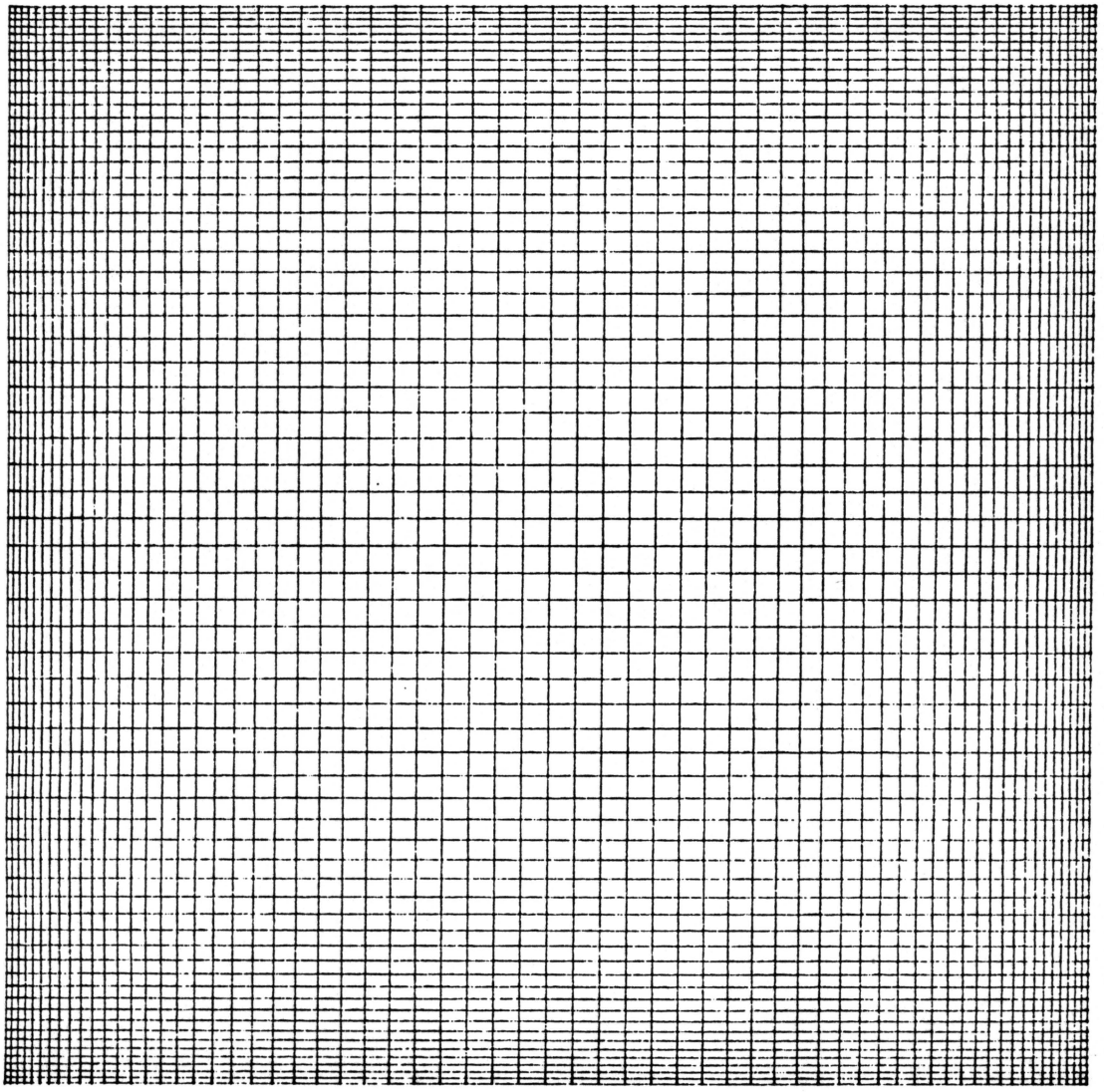

Fig. 6. Representative grid for nonuniform driven cavity
A_o = 1.4, 65 x 65

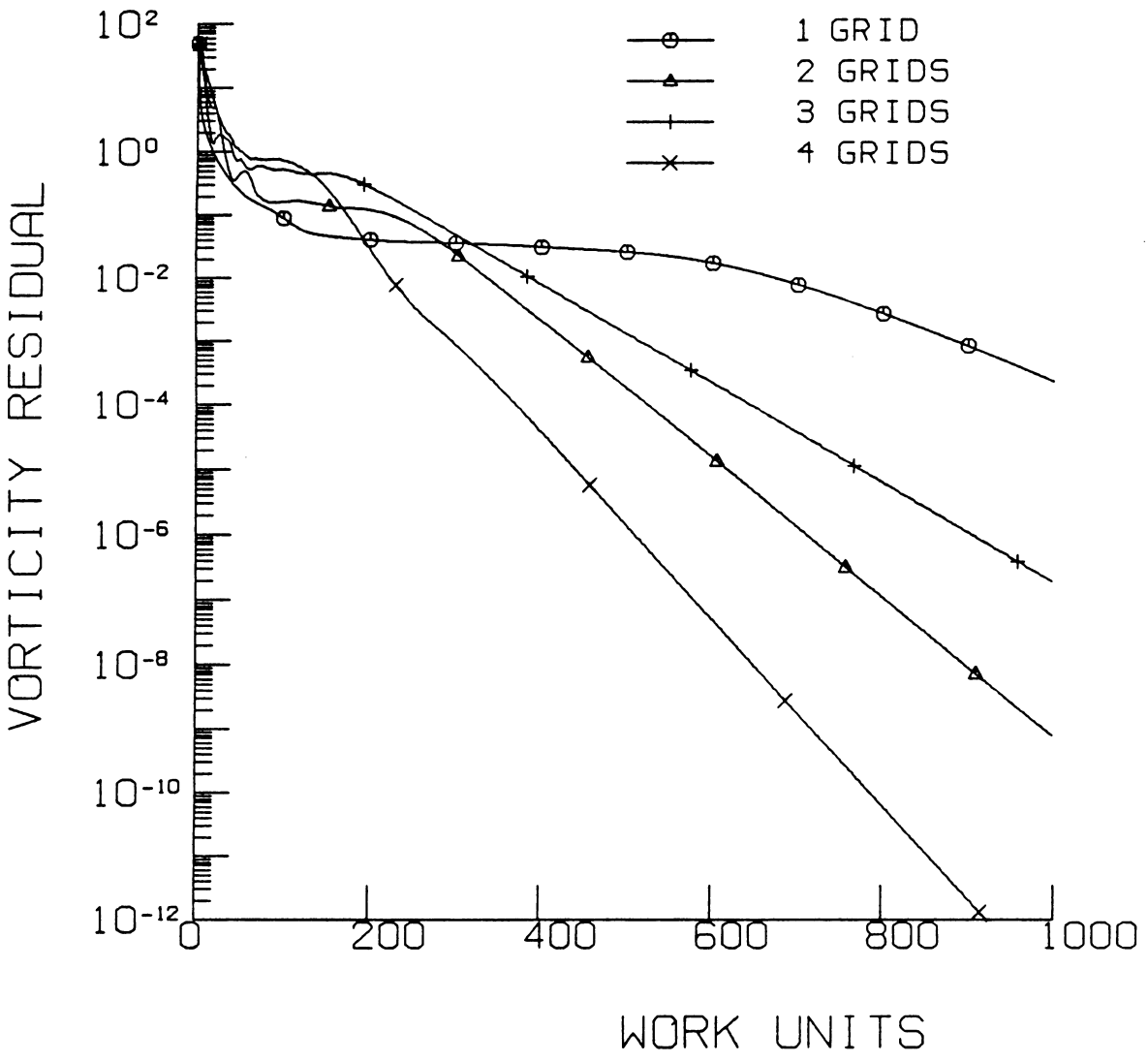

Fig. 7. Convergence history for driven cavity at Re = 1000, nonuniform 65 x 65 grid, $A_0 = 1.4$

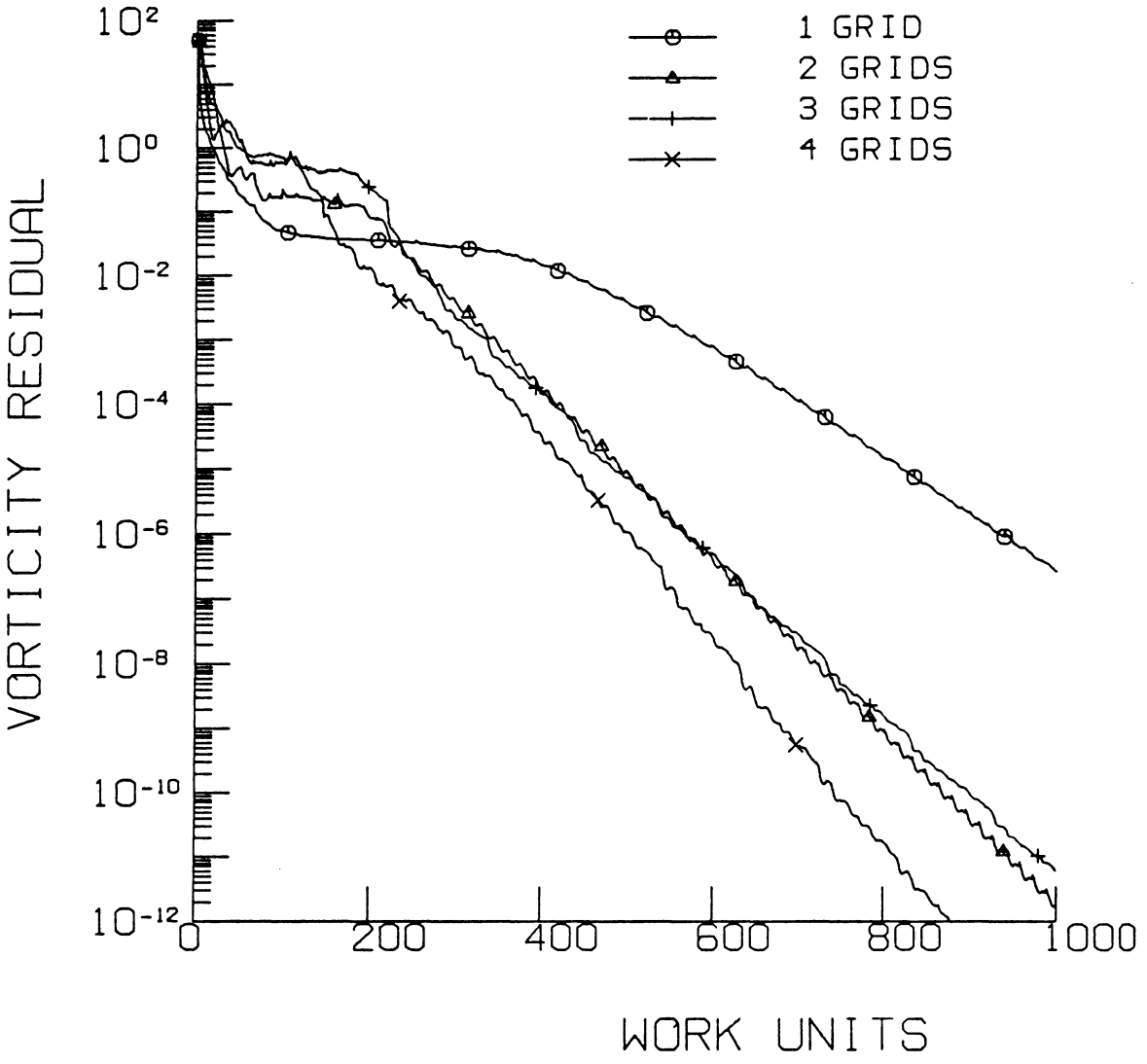

Fig. 8. Convergence history with two-parameter extrapolation for driven cavity at Re = 1000, nonuniform 65 x 65 grid, $A_0 = 1.4$

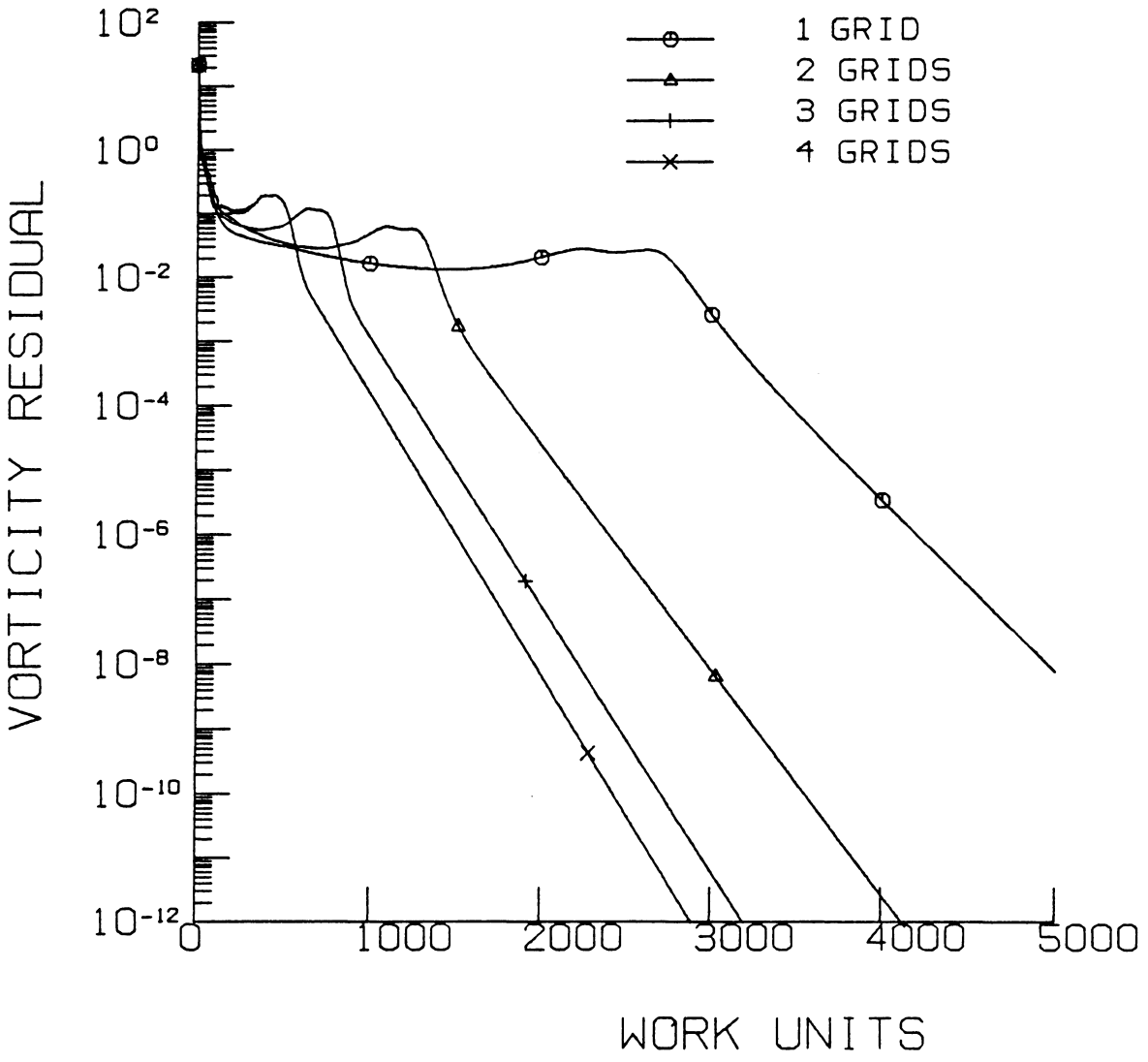

Fig. 9. Convergence history for driven cavity at Re = 3200, nonuniform 65 x 65 grid, $A_0 = 1.4$

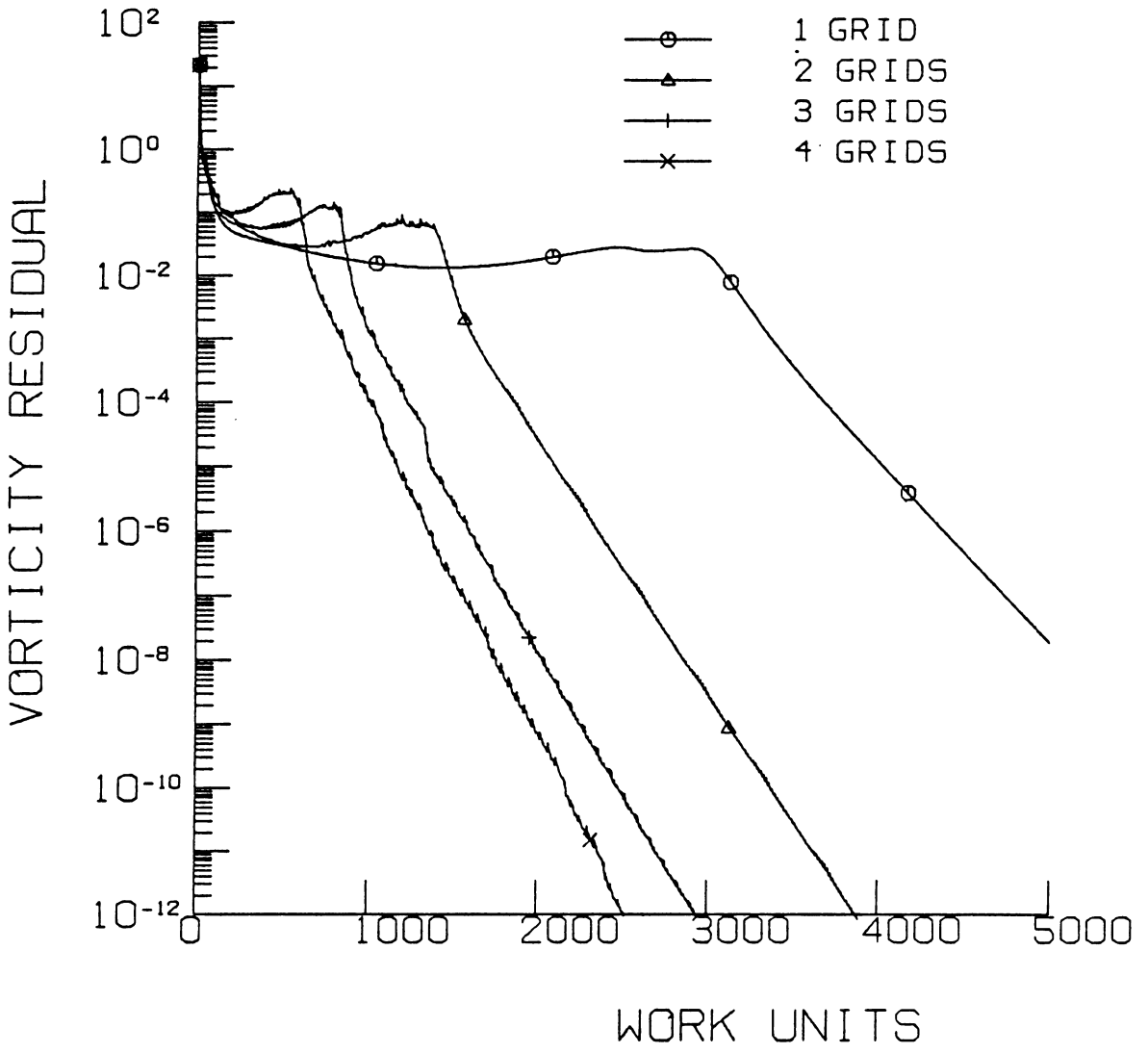

Fig. 10. Convergence history with two-parameter extrapolation for driven cavity at Re = 3200, nonuniform 65 x 65 grid, $A_0 = 1.4$

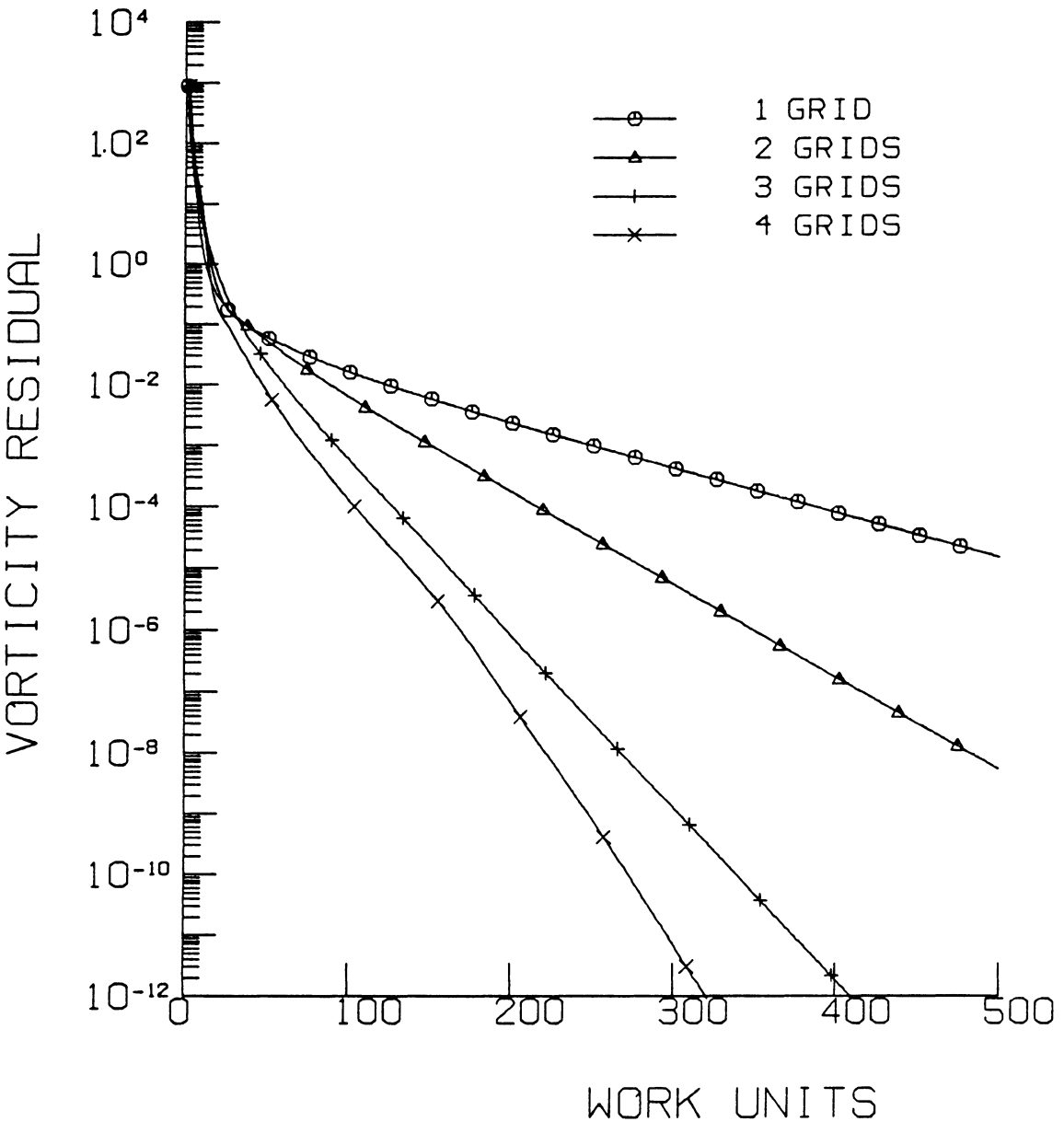

Fig. 11. Convergence history for backward facing step at Re = 200, 49 x 49 uniform grid

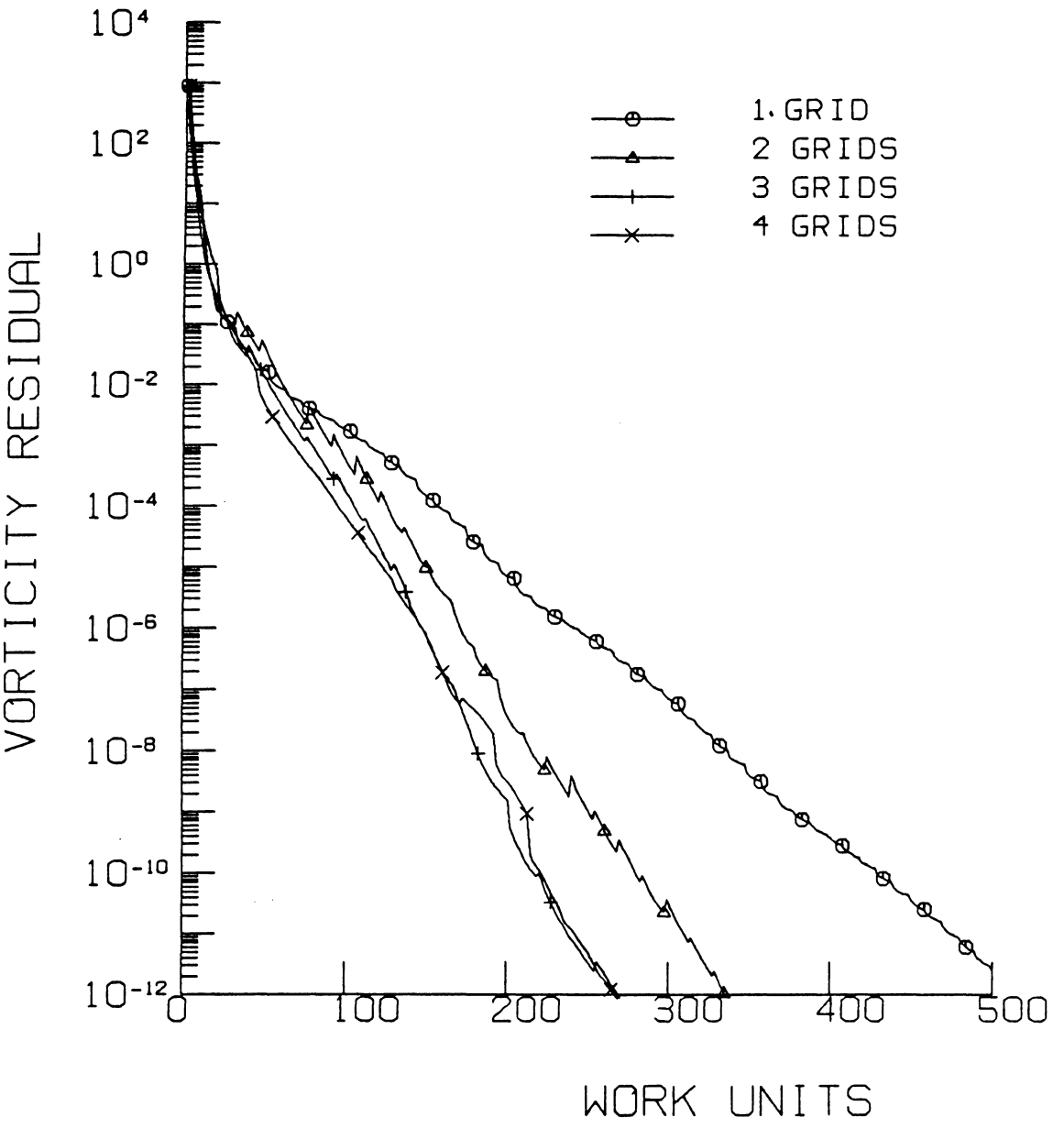

Fig. 12. Convergence history for backward facing step with one-parameter extrapolation at Re = 200, 49 x 49 uniform grid

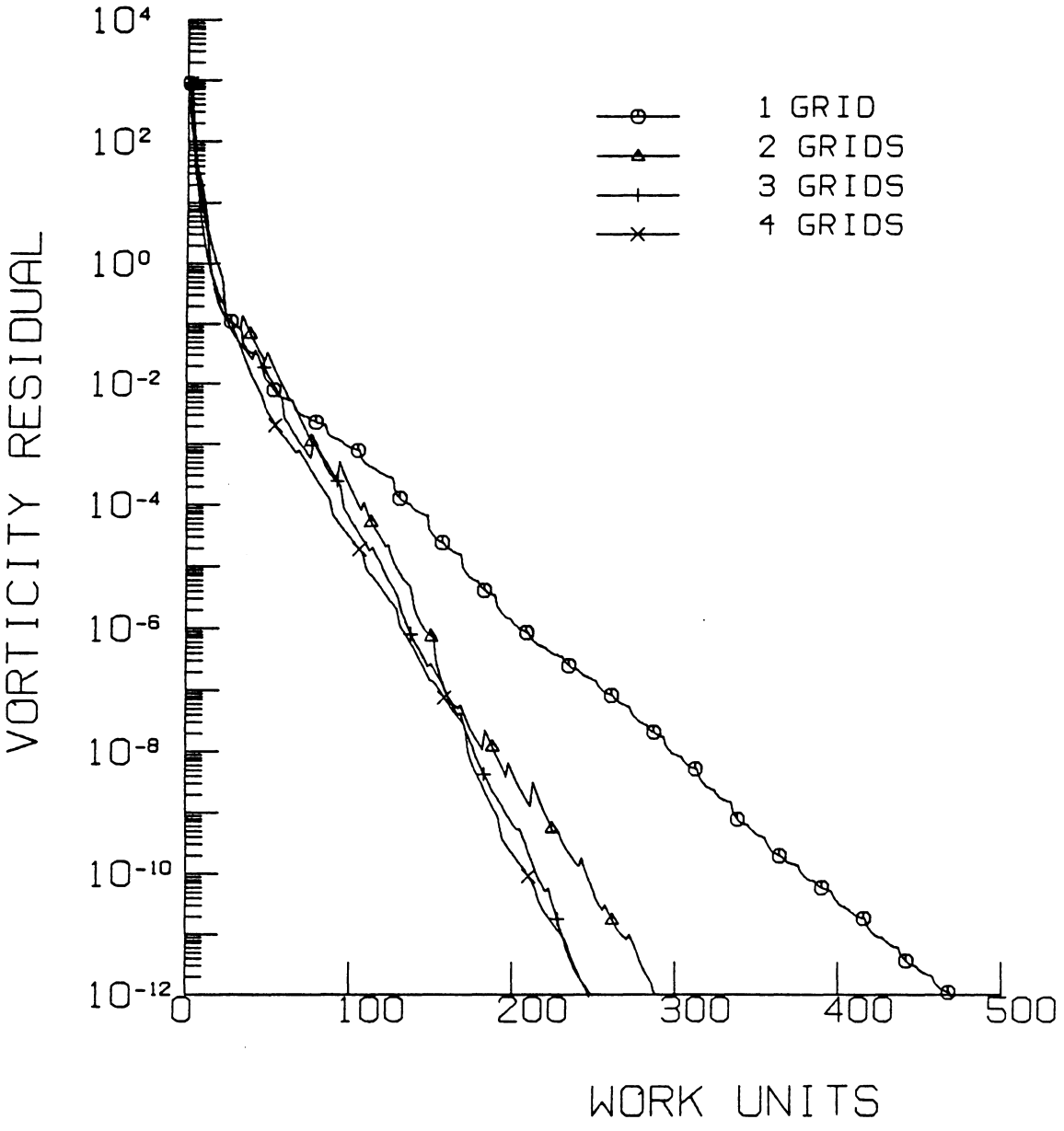

Fig. 13. Convergence history for backward facing step with two-parameter extrapolation at Re = 200, 49 x 49 uniform grid

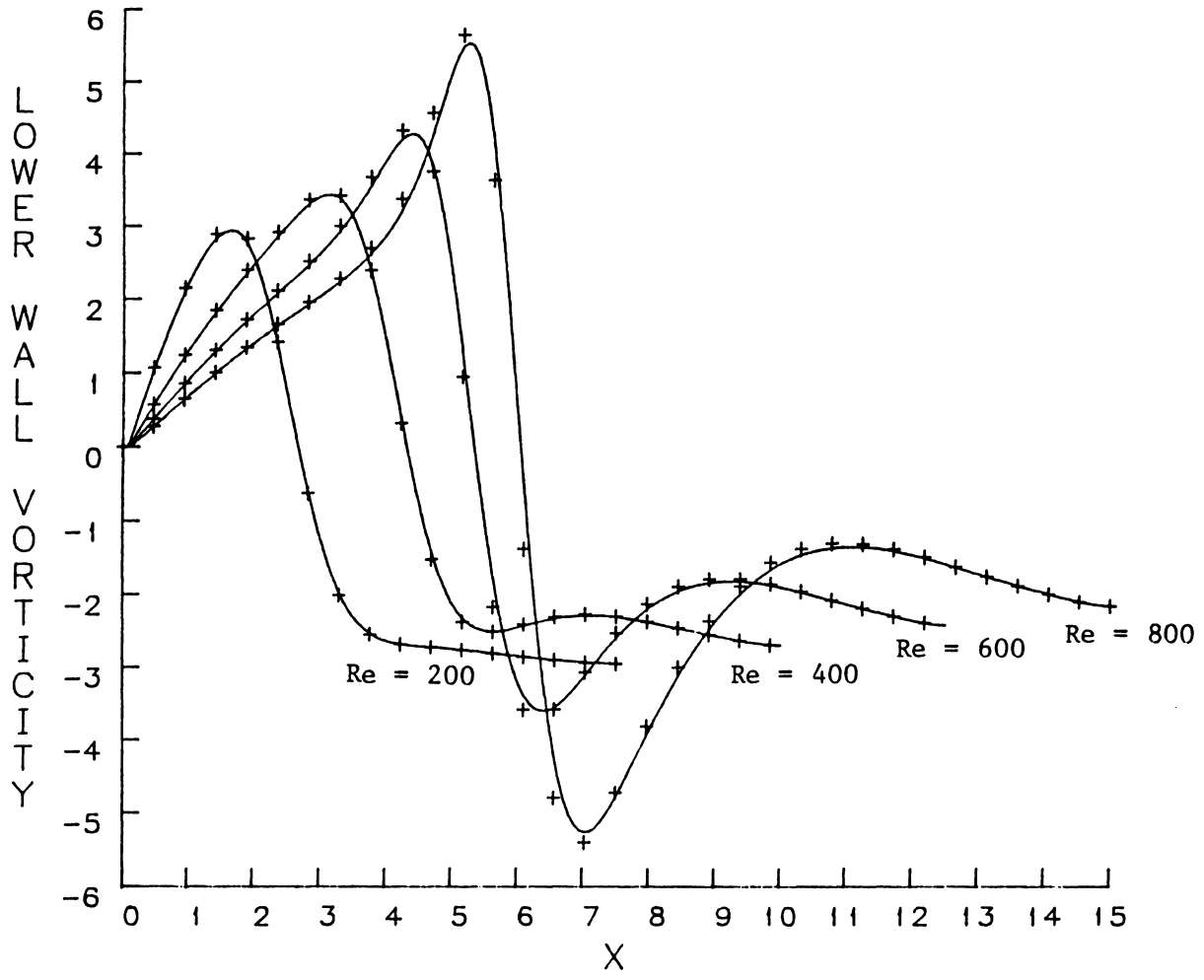

Fig. 14. Lower wall vorticity for backward facing step

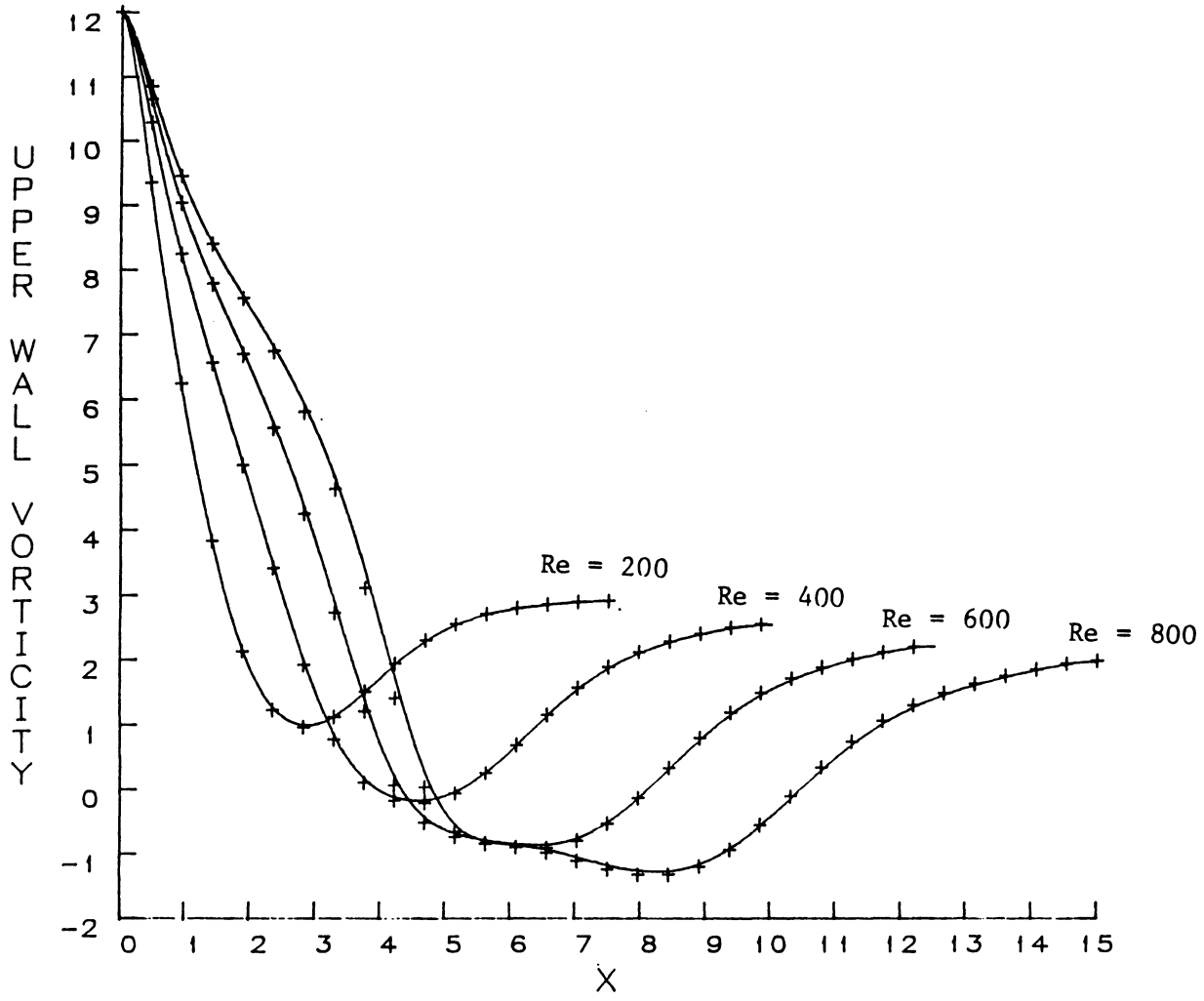

Fig. 15. Upper wall vorticity for backward facing step

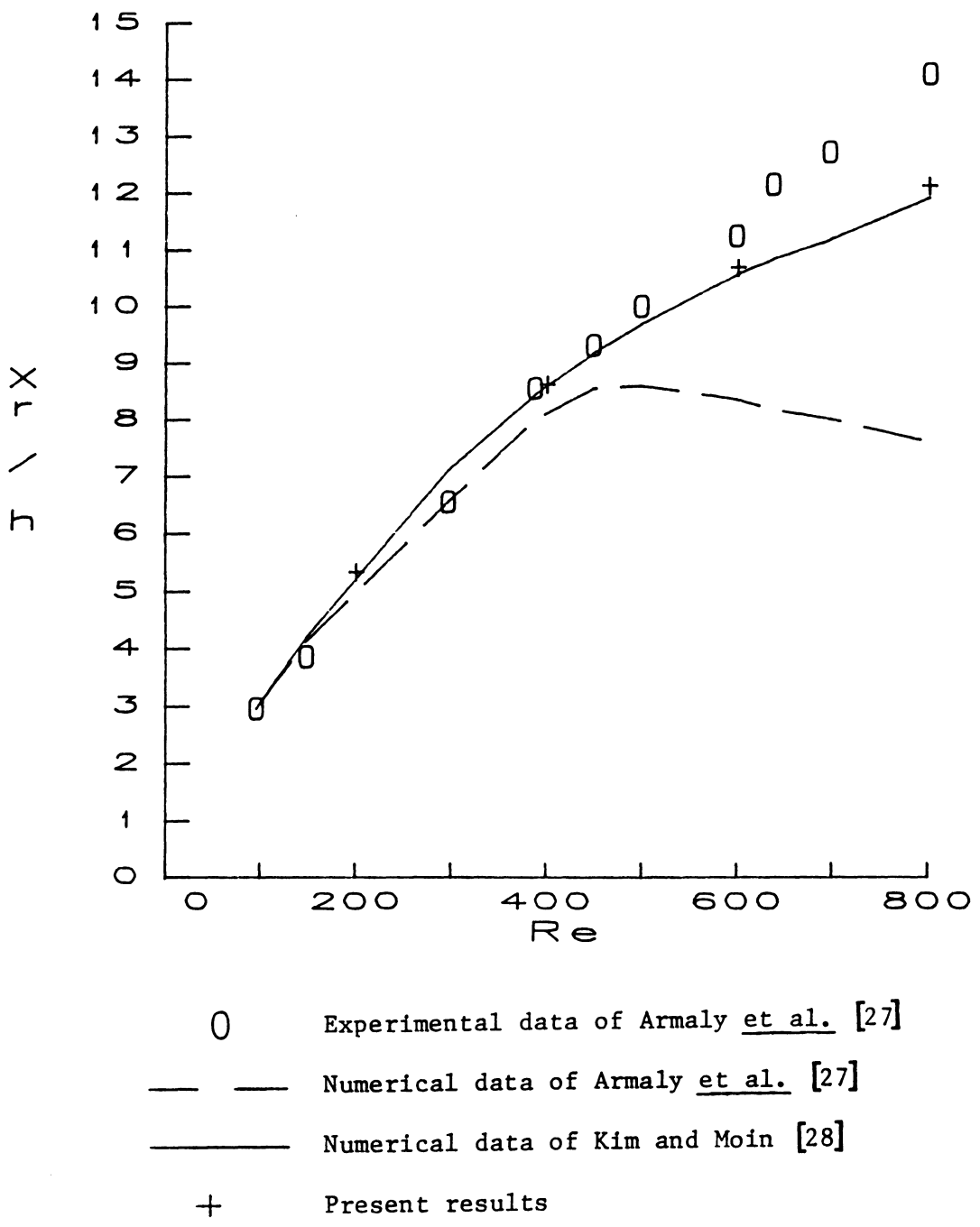

Fig. 16. Reattachment length for backward facing step

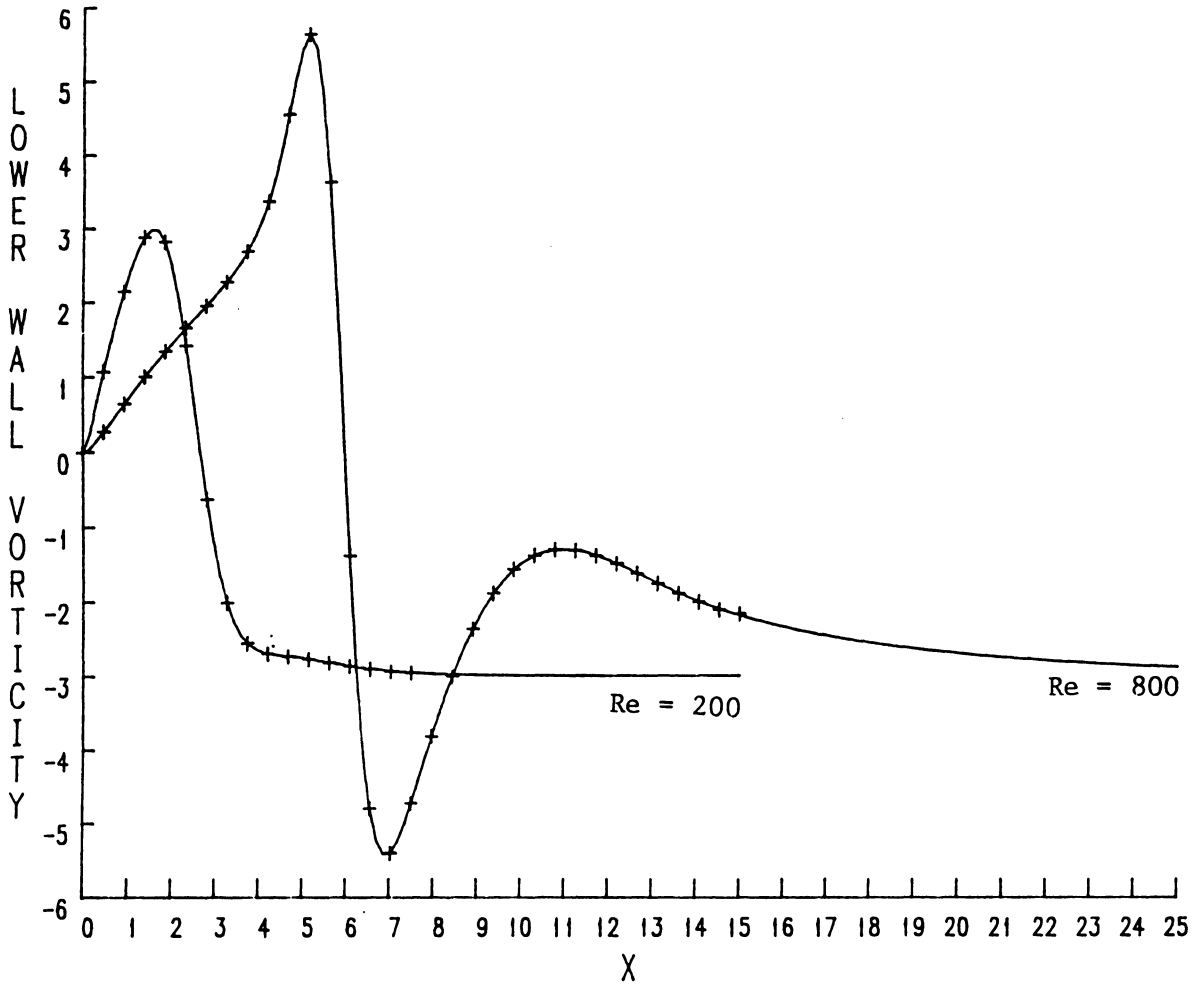

Fig. 17. Lower wall vorticity with extended outflow boundary condition for backward facing step

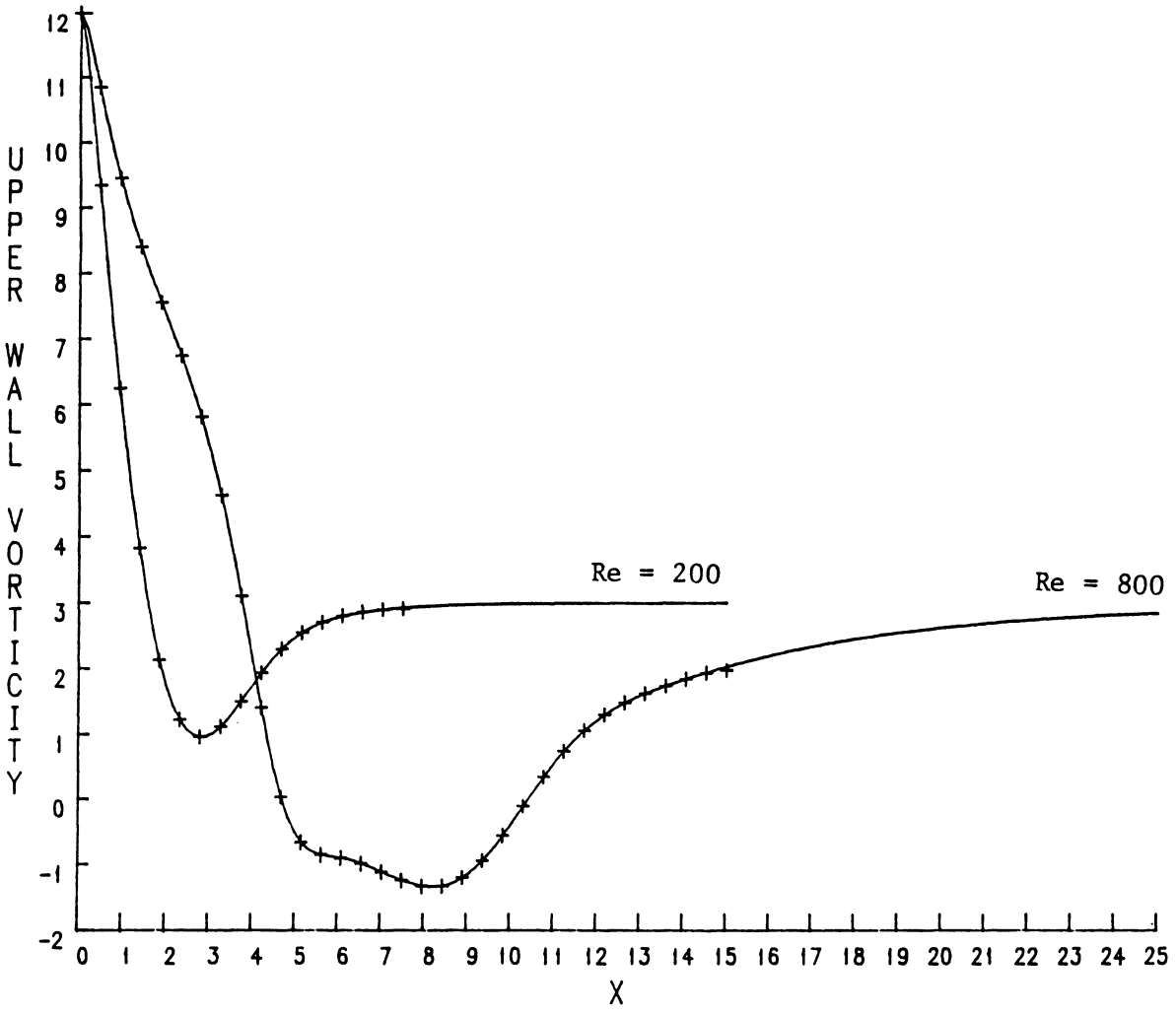

Fig. 18. Upper wall vorticity with extended outflow boundary condition for backward facing step

Table 1. Influence of k on the convergence rate.

k	5	10	15	20
One-Parameter	350.2	365.0	316.6	316.0
Two-Parameter	330.8	287.7	290.6	296.0

Table 2. Numerical results for the driven cavity.

		ψ_M	ω_C
Re = 1000	97 x 97 uniform	.1174	14.95
	65 x 65 nonuniform	.1181	14.88
	Reference 1	.1179	14.89
Re = 3200	97 x 97 uniform	.1166	26.98
	65 x 65 nonuniform	.1193	25.96
	Reference 1	.1204	25.39

Table 3. Separation and reattachment lengths for the backward facing step.

	Re	200	400	600	800
X1R	coarse	5.3263	8.5766	10.5681	11.9343
	fine	5.3357	8.6176	10.6810	12.1018
X2S	coarse		7.7423	8.5118	9.4072
	fine		7.9024	8.6639	9.6059
X2R	coarse		10.5495	16.2225	20.8467
	fine		10.4674	16.2311	20.9281

REFERENCES

1. U. Ghia, K. N. Ghia and C. T. Shin, "High-Re Solutions for Incompressible Flow Using the Navier-Stokes Equations and a Multigrid Method", J. Comp. Physics, Vol. 48, 1982, pp. 387 - 411.

2. A. Brandt, "Multi-Level Adaptive Solutions to Boundary-Value Problems", Math. of Comp., Vol. 31, No. 138, 1977, pp. 333 - 390.

3. R. Schreiber and H.B. Keller, "Driven Cavity Flows by Efficient Numerical Techniques", J. Comp. Physics, Vol. 49, 1983, pp. 310 - 333.

4. S. G. Rubin, "Incompressible Navier-Stokes and Parabolized Navier-Stokes Solution Procedures and Computational Techniques", Lecture Notes for Series on Computational Fluid Dynamics, Von Karman Institute for Fluid Dynamics, 1982.

5. S. G. Rubin and P. K. Khosla, "Navier-Stokes Calculations with a Coupled Strongly Implicit Method - I", Computers and Fluids, Vol. 9, 1981, pp. 163 - 180.

6. H. L. Stone, "Iterative Solution of Implicit Approximations of Multidimensional Partial Differential Equations", SIAM J. Numer. Anal., Vol. 5, No. 3, September 1983, pp. 530 - 558.

7. O. R. Burgraff, "Analytical and Numerical Studies of Steady Separated Flows", J. Fluid Mech., Vol. 24, 1966, pp. 113 - 151.

8. P. J. Roache, Computational Fluid Dynamics, Hermosa, Albuquerque, New Mexico, 1972.

9. S. G. Rubin and P. K. Khosla, "A Diagonally Dominant Second-Order Accurate Implicit Scheme", Computers and Fluids, Vol. 2, 1974, pp. 207 - 209.

10. A. Brandt, "Multi-Level Adaptive Computations in Fluid Dynamics", AIAA Paper No. 79-1455, 1979.

11. A. Brandt and N. Dinar, "Multigrid Solutions to Elliptic Flow Problems", Numerical Methods for PDEs, Ed. J. H. Bramble, Academic Press, New York, 1979, pp. 53 - 147.

12. M. Napolitano and R. W. Walters, "An Incremental Block Line Gauss-Seidel Method for the Navier-Stokes Equations", AIAA Paper No. 85-0033, 1985 also AIAA Journal, to appear.

13. R. M. Beam and R. F. Warming, "An Implicit Factored Scheme for the Compressible Navier-Stokes Equations", AIAA Journal, Vol. 16, April 1978, pp. 393-402.

14. M. Napolitano, "High Re Separated Flow Solutions Using the Navier-Stokes and Approximate Equations", AIAA Paper No. 85-1688, 1985.

15. A. Halim and M. Hafez, "Calculation of Separation Bubbles Using Boundary-Layer-Type Equations - Part I & II", AIAA Paper No. 84-1585, 1984.

16. O. Inoue, "Separated Boundary Layer Flows with High Reynolds Numbers", Lecture Notes in Physics, Vol. 141, 1981, p. 224.

17. D. E. Edwards and J. E. Carter, "A Quasi-Simultaneous Finite Difference Approach for Strongly Interacting Flow", Third Symposium on Numerical and Physical Aspects of Aerodynamic Flows, Long Beach, CA, Jan. 1985.

18. M. Napolitano, "Efficient ADI and Spline ADI Methods for the Steady-State Navier-Stokes Equations", Int. J. Num. Methods in Fluids, Vol. 4, 1984, pp. 1101 - 1115.

19. M. Napolitano, "An Incremental Multigrid Strategy for the Fluid Dynamic Equations", AIAA Paper No. 85-1517, 1985.

20. A. Jameson, "Solution of the Euler Equations for Two Dimensional Transonic Flow by a Multigrid Method", Mathematics and Computation, Vol. 13, 1983, pp. 327 - 355.

21. M. Hafez and H. K. Cheng, "Convergence Acceleration of Relaxation Solutions for Transonic Flow Computations", AIAA Journal, Vol. 15, No. 3, 1977, pp. 329 - 336.

22. M. Hafez, E. Parlette and M. Salas, "Convergence Acceleration of Iterative Solutions of Euler Equations for Transonic Flow Computations", AIAA Paper No. 85-1641, 1985.

23. R. W. Walters and D. L. Dwoyer, "An Efficient Iteration Strategy Based on Upwind/Relaxation Schemes for the Euler Equations", AIAA Paper No. 85-1529-CP, 1985.

24. J. L. Thomas, B. van Leer and R. W. Walters, "Implicit Flux-Split Schemes for the Euler Equations", AIAA Paper No. 85-1680, 1985.

25. B. van Leer and W. A. Mulder, "Relaxation Methods for Hyperbolic Equations", T.H.D. Report 84-20, Delft University of Technology, The Netherlands, 1984.

26. L. Fuchs, "Multigrid Solution of the Navier-Stokes Equations on Non-Uniform Grids", Multigrid Methods, NASA Conference Publication 2202, Proceedings of Symposium held at Ames Research Center, Moffett Field, California, October 21-22, 1981, pp. 83 - 100.

27. B. F. Armaly, F. Durst, J. C. F. Pereira and B. Schonung, "Experimental and Theoretical Investigation of Backward-Facing Step Flow", J. Fluid Mech., Vol. 127, 1983, pp. 473 - 496.

28. J. Kim and P. Moin, "Application of a Fractional-Step Method to Incompressible Navier-Stokes Equations", J. Comp. Physics, Vol. 59, No. 2, June 1985, pp. 308 - 323.

29. K. Morgan, J. Periaux and F. Thomasset (Eds.), "Analysis of Laminar Flow over a Backward Facing Step", Notes on Numerical Fluid Mechanics, Volume 9, Vieweg, 1984.

The vita has been removed
from the scanned document